May 20, 1984

UNITED STATES OF AMERICA
NUCLEAR REGULATORY COMMISSION

BEFORE THE ATOMIC SAFETY AND LICENSING BOARD

In the Matter of	)	
	)	Docket Nos. 50-445 and
TEXAS UTILITIES ELECTRIC COMPANY, ET AL.	)	50-446
	)	
	)	(Application for
(Comanche Peak Steam Electric Station, Units 1 and 2)	)	Operating Licenses)
	)	

AFFIDAVIT OF ROBERT C. IOTTI REGARDING
UPPER LATERAL RESTRAINT BEAM

I, Robert C. Iotti, having first been duly sworn hereby depose and state, as follows: I am Chief Engineer of Applied Physics for Ebasco Services, Inc. In this position I am responsible for directing analytical work in diverse technical areas, including analyses of the response of major structures, piping and support systems to dynamic events, including earthquakes and loss of coolant accidents. I have been retained by Texas Utilities Generating Company to coordinate and oversee the technical activities performed to respond to the Board's December 28, 1983, Memorandum and Order (Quality Assurance for Design). A statement of my educational and professional qualifications was transmitted with Applicants' letter of May 16, 1984, to the Licensing Board in this proceeding.

Q1. What is the purpose of this affidavit?

A1. The purpose of this affidavit is to respond to the Licensing Board's conclusion in its December 28, 1983, Memorandum and Order (at 56) that "in the face of the possibly conflicting engineering viewpoints of three different parties, we conclude that Applicant has not demonstrated the adequacy of its analysis of the upper lateral restraint beam." Accordingly, Applicants have prepared detailed finite element analyses to demonstrate the adequacy of the upper lateral restraint beam and of the associated reinforced concrete supporting walls. The results of these analyses confirm that the design of the restraint and the concrete walls which would be affected by the assumed accident conditions is adequate to withstand the postulated loads which are pertinent to this analysis.

Q2. Can you summarize the analyses which have been performed?

A2. This investigation was performed to determine the effects of a LOCA break on the upper lateral steam generator restraint and associated steam generator compartment walls from the thermal growth of the restraint, as well as from concurrent loads and other environmental effects which would occur during a postulated LOCA. In addition, although only the effects of a LOCA on the upper lateral restraint were discussed during the licensing hearings, it was recognized that the lower lateral restraint (approximately 24 feet below the upper and serving a similar function) would

likewise experience and cause similar and simultaneous effects elsewhere in the compartment. Therefore, the investigation was expanded to include the lower restraint to assure that the most significant effects were addressed, i.e., their overlapping effects.

Q3. Please describe the analytical methodology that was used.

A3. First we wish to define the extent of the geometry of the problem that was modelled.

The boundaries of the analysis were established as a section of the reactor building internal structures consisting of steam generator compartments 1 and 4 between elevation 819' (close to the top of the mat and 15' 10" below the lower lateral restraint) and elevation 883' (24' above the upper lateral restraint). Elevation boundaries were selected to assure that all stiffness contributions to the restraining walls from adjacent floors and walls were properly accounted for. Boundary limitations of the analysis (beyond compartments 1 and 4 defined in Appendix II Figures 1 & 2) were determined from the original finite element analysis of the internal structures, done as part of the original design effort on the internal structures. Figures 1, 2, 3, 4 and 5 of Appendix II (attached) show the portions of the internal structures included in the present analysis.

Next we describe the finite element model employed. The analysis of the upper and lower lateral restraints and compartment walls was performed using NASTRAN. The particular version of NASTRAN used has the capability to determine the cracking propagation in the concrete due to the interaction of thermal and mechanical loads. The crack development and propagation is determined by means of a nonlinear iteration technique. The program provides, as an output, stresses in the reinforcing steel, stresses in the concrete, displacements, forces and moments in the finite elements, crack pattern for the structure used in the model. Appendix III (attached) provides a summary description of the theory employed in the solution method of the version of NASTRAN used for this analysis. This version has been verified and has been reviewed by the NRC in other applications.

The finite element model of the structure is generated using triangular and quadrilateral layered shell elements and beam elements. Two bounding analyses have been performed. The first analysis provides the upperbound on the effects on concrete walls. For this analysis no credit is given to the tensile capacity of the concrete. This is consistent with ACI Code design requirements which assume concrete has no tensile capacity. However, concrete tensile strength can be approximately 10% of f_c and will add to the compartment wall system stiffness until cracking initiates.

Therefore, to assess the maximum loads on the beam, a value of 450 psi for concrete tensile capacity was used in the second analysis. This value is about 10% of the concrete strength actually produced at CPSES but it is 12.5 percent of the concrete strength used in the analysis. Applicants have used the higher figure for conservatism as explained later. Plots of the finite element models employed in the analyses are shown in Figures 1 through 19 of Appendix IV.

Q4. What type of loads were input into the finite element model?

A4. For purposes of these analyses, it was assumed that compartment pressure and temperature effects due to LOCA, would occur in combination with seismic loads. Mechanical loads, such as thrust load reacted by the steam generator restraints and jet impingement were taken at their maximum peak values in combination with maximum differential pressure although consideration of their time histories would have permitted significant reductions in mechanical loads. Further, although discussion at the hearings centered on effects of a LOCA, Applicants considered that a main steam line break would result in higher compartment temperatures than a LOCA break and might have a more significant impact on thermal stresses. Accordingly, the analyses were further expanded to calculate the temperatures, pressures and associated stresses in the compartment walls and restraints due to a main steam line break. For the main steam line break analysis, however,

seismic loads were not assumed to occur simultaneously with mechanical and thermal loads caused by the break. This is consistent with the position taken by the NRC staff in NUREG-138,[1] which states: "consistent with the lesser importance of the secondary system boundary, the Staff does not require that an earthquake be assumed to occur coincident with a postulated spontaneous break of the steam line piping."

The temperature and pressure effects and postulated loading conditions for both the LOCA and main steam breaks are as follows:

1. LOCA - The assumed critical break for purposes of this analysis is conservatively assumed to be a full double ended break at the reactor coolant pump suction on the reactor coolant loop. (Note that because of the primary system supports/restraints, this large a break cannot occur.) This break has been chosen because it provides the highest mass and energy flow rates into the compartment and results in the largest mechanical loads, the largest differential pressure across the walls and the highest LOCA temperatures. Figure 1 of Appendix I (attached) shows the time history of each of the noted effects. It can be seen that all mechanical loads reduce to zero in less than 0.5 seconds.

---

1 NUREG-138, "Treatment of Non-Safety Grade Equipment in Evaluations of Postulated Steam Line Break Accidents," November, 1976.

Differential accident pressure across the walls rises rapidly to a maximum of 24 psi at 0.5 seconds and is reduced to essentially 0 after approximately 4 seconds. For purposes of computing maximum differential pressure, the temperature in the compartment is assumed to be at 120°F. at the time of the LOCA. However, to compute the resulting effects, a temperature of 70°F is employed in the analysis. Both of these assumptions contribute to the conservatism of the results. The former maximizes the compartment pressure and temperature (hence the loads seen by the walls and beam). The latter maximizes the response of the beam and walls. Although the temperature of the atmosphere inside the compartment rises very rapidly, the temperature in the steel beams and concrete lag behind. For the restraints of interest the average temperature rises to a peak of 282°F. for the upper restraint (289°F. for the lower restraint) after 216 seconds and diminishes thereafter.

The temperature rise in the restraints has been computed by the finite difference computer program HEATING 5 Version 2. Input compartment atmosphere temperature histories to these heat transfer analyses have been developed via a multinodal compartment

analysis which utilizes RELAP 4 Mod 5. Schematics of the models used for these analyses are shown in Appendix V.

Based on the above, two postulated loading conditions were considered for LOCA, as follows:

Stage 1 - At 0.5 seconds after the break/time of maximum pressure

a. Maximum differential pressure across walls = 24 psi

b. Coincident accident temperature of beam
   = 128°F. (upper beam)
   = 133°F. (lower beam)

c. Peak mechanical loads were used in the analyses even though they occur at earlier times. Mechanical loads refer to thrusts imposed by steam generator restraints, loads imposed by reactor coolant pump restraints and jet loads due to the postulated pump suction break. The thrust loads include both reaction loads to the break and seismic (full SSE) loadings from the primary system which are transmitted via the steam generator and reactor coolant pump restraints.[2] (Actual peak mechanical loads occur at 0.2 seconds and are zero at 0.5 seconds and hence have been included conservatively.)

d. Seismic loads generated in all the structures, restraint beams, major components from the SSE are included coincidentally.

---

2 Seismic reaction loads from the primary system seismic response are overestimated since the structural model also includes masses of steam generator and pump, already included in the Westinghouse seismic model which produced seismic reaction loads at structural interface.

Stage 2 - At 216 seconds after the break (time of maximum temperature) on upper lateral support

a. Maximum accident temperature of the beam[3]
= 282°F. - upper beam
= 289°F. - lower beam

b. Coincident differential pressure across walls = 1 psi even though thermo-hydraulic analyses indicate no differential pressure.

c. In this instance the reaction load of the beam to the seismic excitation of the primary system had not been initially included in the NASTRAN analyses with the intent to maximize the reaction loads from beam thermal constraint and to maximize beam stresses. The stresses resulting from the reaction were computed separately and added in the most conservative fashion to the stresses generated by the NASTRAN analysis. Structural seismic loads, seismic loads or walls due to beams, steam generators and pump masses excitation are included. To verify the conservatism of this approach, Applicants have run the worst case problem (i.e. LOCA Peak Temperature with concrete tensile strength equal to 450 psi) including the primary system seismic load. The results of this analysis are also shown in Tables 1 & 2 and they confirm that conservatism of the analysis.

2. Main Steam Line Break - The assumed critical break for purposes of this analysis is a split break at 30% power at the steam generator outlet nozzle. This break was selected as the critical break because it results in the highest temperature in the compartment from the

---

3 Actually, the maximum actual temperature of 289°F. in the lower beam occurs at 144 seconds (approximately 285°F. at 216 seconds) but has been assumed to occur simultaneously with the maximum in the upper beam at 216 seconds.

array of breaks considered, which included full double ended and split breaks for full, 70% and 30% power levels.

Figure 2 of Appendix I contains time history plots of the effects of the main steam line break. It can be seen that a small but negligible pressure spike of 0.08 psi occurs in the compartment at 1.0 seconds and dissipates by 3.0 seconds. Also, all mechanical loads are reduced to zero within 0.5 seconds. Temperature in both upper and lower lateral supports rises to approximately 355°F. at about 300 seconds. A more preliminary and conservative figure of 370°F. was used in the actual analysis.

Based on the above, the postulated loading condition for the main steam line break is as follows:

a. Maximum average temperature of the upper and lower lateral restraints = 370°F.

b. Coincident differential pressure across walls = 1 psi used even though analyses indicate that it is zero.

c. Mechanical loads: none used since seismic loads are not combined in this analysis, and other mechanical loads (i.e., steam line break reaction loads) are negligible at the time of peak temperature.

Q5. What are the results of the analyses?

A5. We would like to discuss the results of impact on the concrete structures and on the beams separately. First we address the impact on the concrete structure.

NASTRAN analysis for the concrete structures was conducted for zero concrete tensile strength and for 450 psi concrete tensile strength. The 0 psi value corresponds to the conventional approach in design which assumes that the concrete has no tensile capacity and hence tends to yield conservative results with regard to concrete and steel stresses. Under laboratory conditions, concrete has been shown to have tensile strengths in the range of 8 to 12% of its compressive strength with 10% being an average. The 450 psi corresponds to 12.5% of the compressive strength of the concrete utilized in the analysis. It is used because it represents 10% of the actual minimum compressive strength of the concrete achieved at CPSES. Applicants recognize that for consistency, with the use of the 4000 psi design strength employed in the analyses, a more appropriate value would have been 400 psi. Further, it should be recognized that under actual field conditions, the chances of achieving perfect bond and continuity between various concrete pours and joints is considered to be remote, consequently it is not likely that the full potential tensile strength could be developed throughout the structure. Thus, 450 psi is considered to represent an absolute upper bound estimate of

the tensile strength of concrete at CPSES. Applicants chose this value so that there could be no question on the conservatism of the reaction loads produced by constraint of thermal expansion of the beam restraints. Another beneficial effect that has been ignored so as to overestimate the reaction loads is the heating of the inner surface at the concrete walls surrounding the compartment during the accident. This surface heating would tend to introduce compressive stresses at the inner surface and tensile stresses at the outer surface. The latter could lead to cracking and additional relief.

The results of the analyses for the concrete structures are set forth in Table 1. As indicated therein, calculated stresses in the concrete and reinforcing steel for both 0 and 450 psi assumed values of concrete tensile strength are well below the conservatively established allowable for mechanical loads.[4]

The following interpretations should be placed on the values listed in the Table:

---

4 The allowable stresses indicated are conservatively based on loads which are mechanical type (non self-limiting) loads. All the actual stresses shown are well within these elastic limits. However, when considering a load combination which includes a faulted, displacement limited effect such as the restraint of the free end displacement of the steel beam, a strain excursion beyond yield into the plastic steel range is acceptable, provided there is no loss of function of any safety related system. When considering such self-limiting effects, the appropriate factor of safety is based on strain rather than stress; this is the basic philosophy behind the ASME Code NF-3231.1 not requiring any calculations to be made for such thermal effects on a steel support frame.

Max. Reinforcing stresses are tensile stresses.

Max. concrete stresses are compressive stresses unless they are indicated as shear stresses.

Thrusts are positive if applied by the beam toward the wall (compression in beam) and negative if away from the wall (tension in beam).

Displacement of the wall at beam end is positive when beam displaces toward the wall and negative when beam displaces away from wall.

Q6. What about the impact on the beams?

A6. The primary purpose of the upper (and lower) lateral restraint beams is to provide restraint to the steam generator during a design basis accident due to the postulated breaks in the primary coolant loop and the main steam lines. The reaction loads from the breaks assumed in the present analyses exist for less than 0.5 seconds, during which time the stress which is caused by constrained expansion of the beam following the increase of temperature within the compartment due to the pipe break, is negligible (see Appendix I, Figures 1 and 2, Plots 1 and 2). During the time in which the constrained expansion stress builds up to its maximum (in the next few minutes), the beam has already served its primary function of resisting the broken pipe thrust.[5] There are thus two different stages to be

---

5 Of course, even if the thermal stress was coincident with the mechanical load, it could be neglected. See FSAR

(footnote continued)

TABLE 1

Item	Conc. Tensile Strength = 0 psi			Conc. Tensile Strength = 450 psi			
	LOCA Peak Press. at 0.5 Sec.	LOCA Peak Temp.	M.S. Peak Temp.	LOCA Peak Temp. 1	LOCA Peak Temp. 2	M.S. Peak Temp.	Notes* See Footnote 5, p. 12
1. Max. Rebar Stress (ksi)	22.0	13.7	17.1	11.4	14.06	20.7	Allowable
Location (Element No.)	(137)	(1475)	(1475)	(1734)	(1734)	(1734)	54 ksi (.9fy)
2. Max. Concrete Compressive Stress (ksi)	0.83	0.91	1.23	1.21	1.41	1.88	Allowable
Location (Element No.)	(1023)	(1389)	(154)	(2125)	(2125)	(2125)	3.4 ksi = .85 f'c
3. Max. Strain In Rebar	0.00076	0.00047	0.00059	0.00039	0.00049	0.00071	Yield strain = .00207
4. Max. Thrust							
Upper (kips)	-2138	1591	2178	3892	3414	4918	
Lower (kips)	156	2350	3210	2909	2868	3988	
5. Total Expansion of Lateral Restraints Upper/Lower (in.)	.138/.099	.21/.14	.29/.19	.16/.06	.17/.06	.25/.08	
5a. Displacement At External Wall End Upper/Lower (in.)	.143/.046	.11/.06	.12/.08	.07/.04	.07/.04	.07/.05	
5b. Displacement At Reactor Wall End Upper/Lower (in.)	-.005/.053	.1/.08	.17/.11	.09/.02	.10/.02	.18/.03	

1 - Analysis purposely excludes primary system seismic loads to maximize beam thrust.

2 - Analysis includes primary system seismic loads

considered. Initially the beam and walls will be exposed to the maximum mechanical loads. Later on the beam will impose the most severe thermal expansion constraint loads. Applicants have analyzed the stresses in the beam at these two different stages: (1) when the mechanical loads peak at 0.5 sec.; (2) when the beam temperature peaks during LOCA. The conditions assumed for the first stage analysis (simultaneous occurrence of maximum effects of mechanical (thrust), seismic, and differential pressure loads) are extremely conservative and bounding. The conditions shown for the second stage are also bounding as a result of imposing the most severe thrust expansion constraint. Intermediate times would result in lower overall loads since differential pressure and mechanical (thrust) loads decay far more rapidly than the temperature rises within the compartment.

As previously stated two analyses have been in fact conducted for the latter stage. One neglects the reactor systems seismic loads reacted by the restraint in order to

---

(footnote continued from previous page)
Section 3.8.3.3.3, 2(b) which states, "thermal loads are neglected when they are secondary and self-limiting in nature and when the material is ductile." This steel beam satisfies these requirements and this is why the thermal loads were originally neglected. See also NRC Standard Review Plan, Section 3.8.3 (page 15), which also allows thermal stresses to be neglected. Even, if this support were classified as ASME-NF, the ASME's philosophy in this regard, is also to neglect such thermal stresses. See ASME Code Section NF-3231.1(c) (faulted condition) and also NF-3231.1(a) and (b) (normal, upset and emergency conditions).

maximize the axial loads experienced by the beams. The other included those loads. Seismic excitation loads for all the structures (including the beams) are always included in the analyses for both stages.

For the steam line break analysis Applicants only analyzed the effects of peak temperature in compartment. Since there is negligible differential pressure within the compartment from a main steam line break, the initial stage results would be bounded by the LOCA initial stage results.

The following Table 2 shows the stresses in the beam and clearly indicates that, even though the beam has already performed its function and is no longer required when the temperature reaches its peak, the stresses in the beam due to the peak temperatures are well within the allowables.

TABLE 2

Loading Condition	Max. Stress in the Upper Lateral Beam*		Allowable
	Concrete Tensile Strength = 0	Concrete Tensile Strength = 450 psi	
1) When mechanical load peaks at 0.2 sec.	18.4 ksi	(not run)	45 ksi (90% Fy)
2) When beam temperature peaks during LOCA	16.85* ksi (7.1)**	22.75 ksi/16.3+ ksi (13.0)**	45 ksi
3) When beam temperature peaks during M.S. line break	8.4 ksi	15.7 ksi	45 ksi

Q7. What do you conclude from these analyses?

A7. In summary, Applicants conclude that (1) the upper and lower lateral restraint beams are adequately designed; and (2) the stresses in steam generator compartment walls are well within the allowable stress and strain limits when the thrusts from the upper and lower lateral beam due to maximum accident thermal loads are applied to the walls.

---

* Primary system seismic load contribution separately calculated and combined with other loads computed from computer analysis.

\+ Computed by NASTRAN program when primary system seismic load is included directly in analysis.

** Numbers in parentheses are results achieved when model is executed without primary system seismic load contribution.

Robert C. Iotti

Sworn to before me this 20th day of May, 1984.

Notary Public

My Commission Expires January 31, 1985

(*) PEAKS OF VARIOUS RESTRAINTS/ SUPPORT LOADS OCCUR AT DIFFERENT PERIODS OF TIME - HOWEVER THEY ALL DISSIPATE WITHIN A PERIOD OF 0.5 SEC.

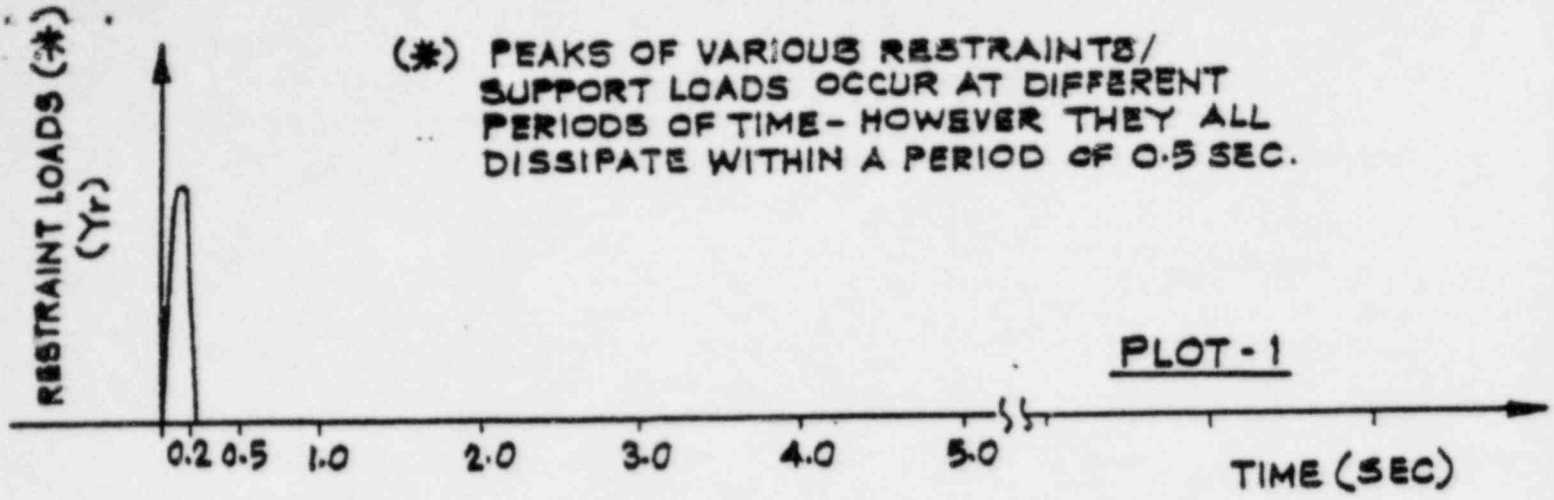

PLOT - 1

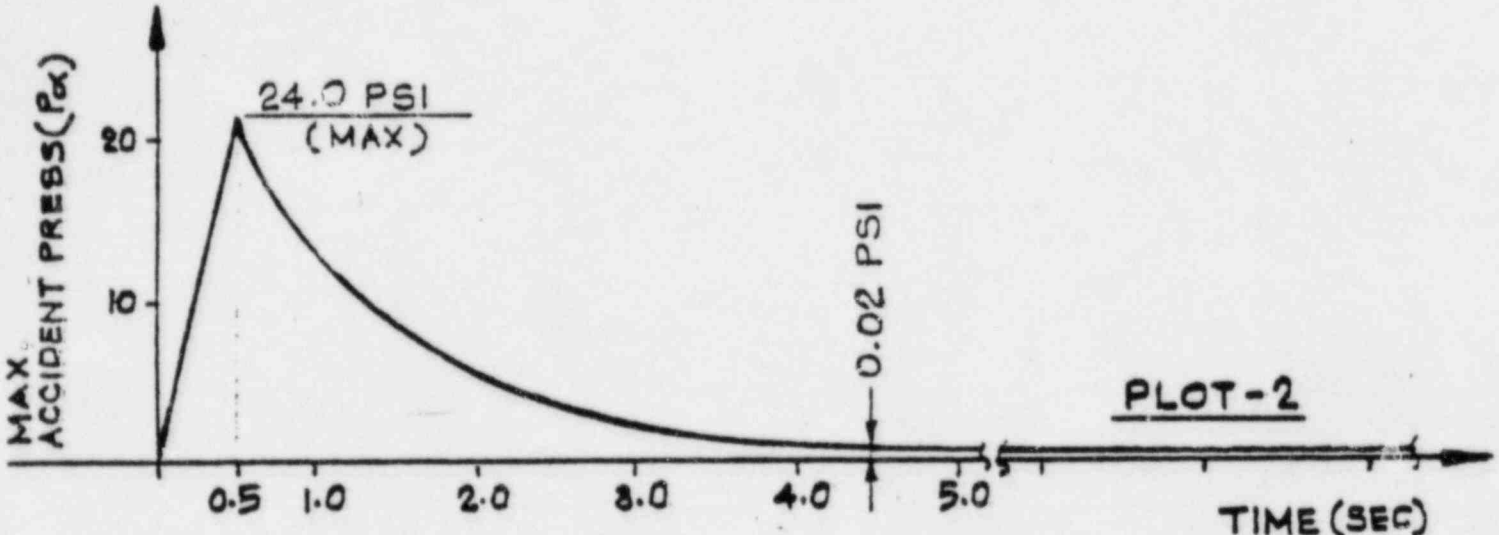

PLOT - 2

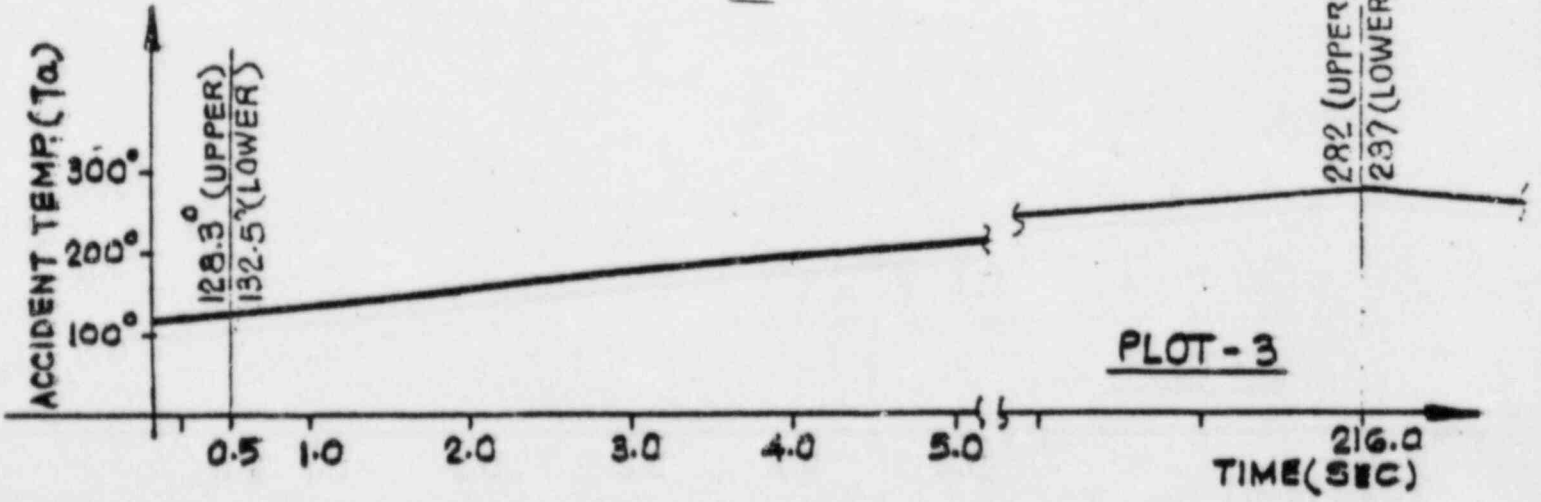

PLOT - 3

R.C. PUMP SUCTION BREAK

PLOT-1 : FROM WE WPT-6987 & WPT-6668
PLOT-2 : FROM MECH. CALC. 511-12A, REV. 0
PLOT-3 : FROM MECH. CALC. 511-12A, REV. 0

APPENDIX I
FIGURE - 1

4.13.84

(*) PEAKS OF VARIOUS RESTRAINTS/ SUPPORT LOADS OCCUR AT DIFFERENT PERIODS OF TIME - HOWEVER THEY ALL DISSIPATE WITHIN A PERIOD OF 0.5 SEC.

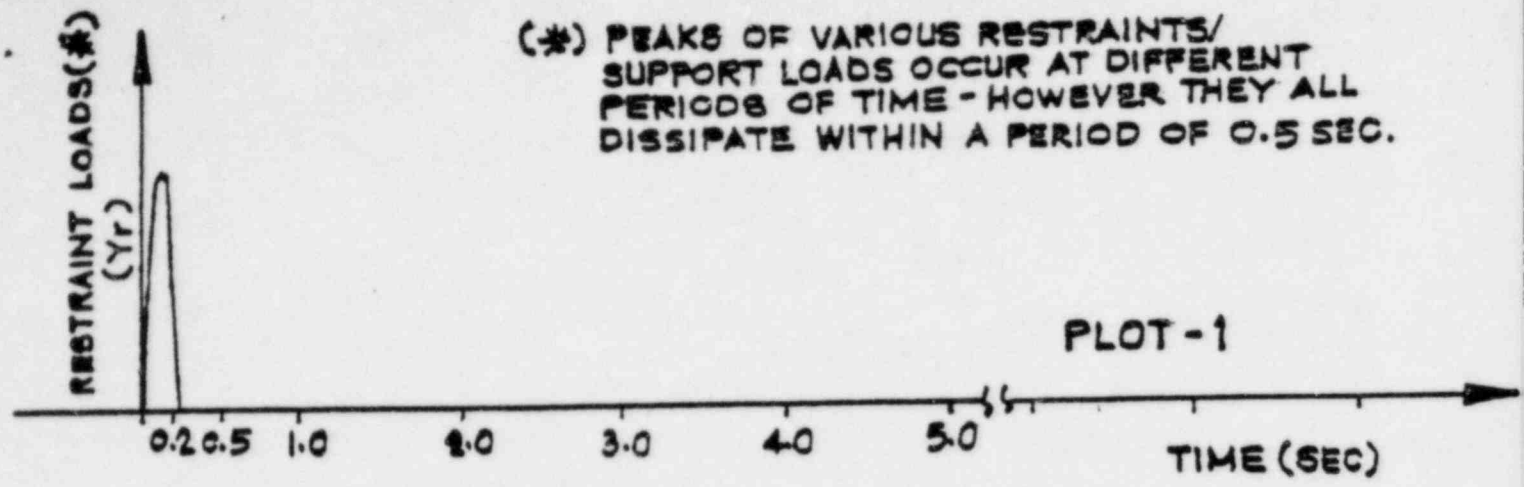

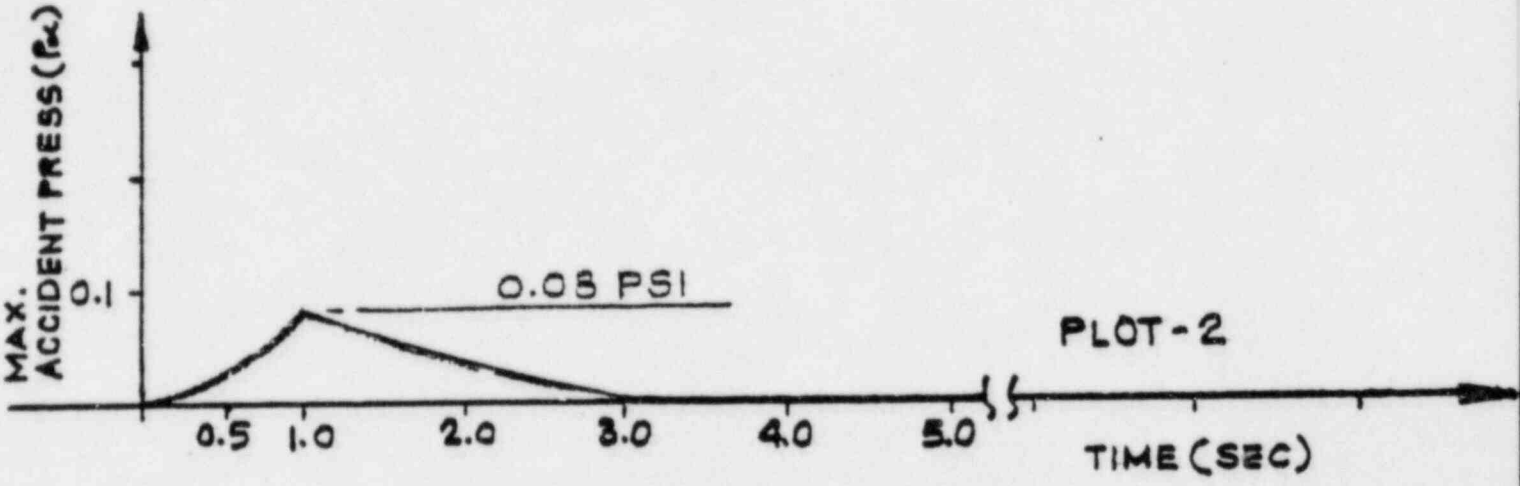

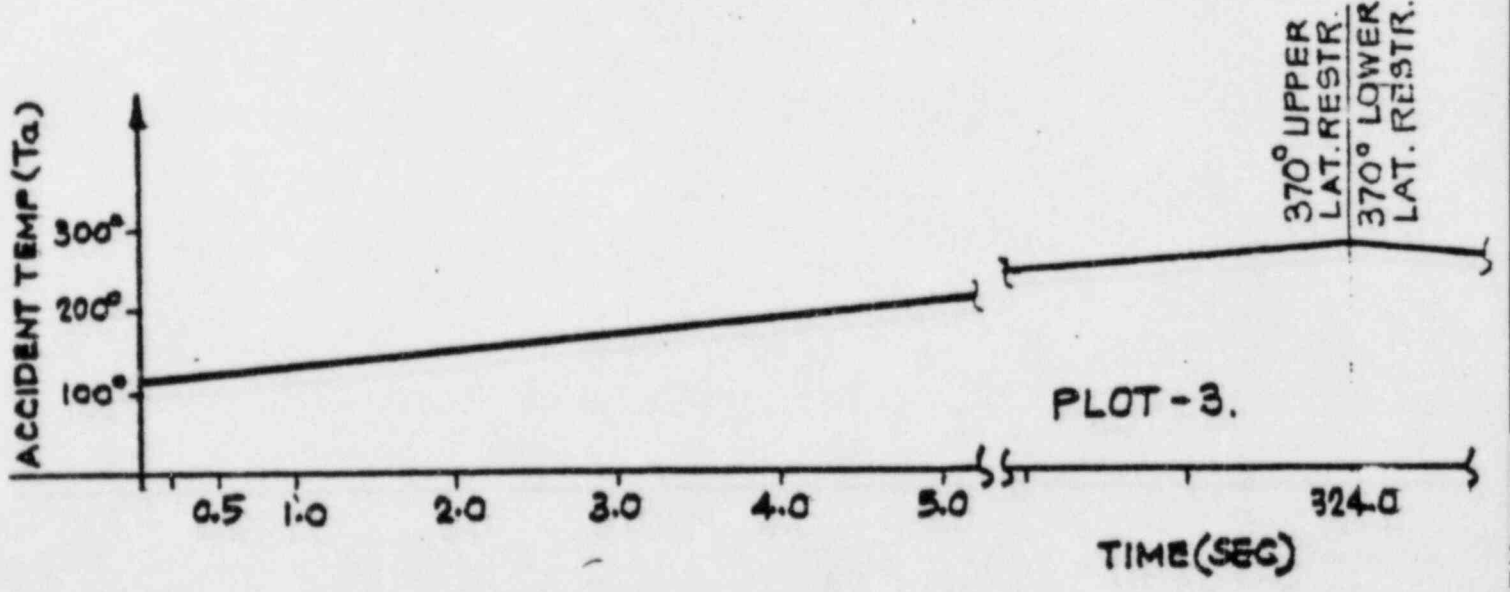

MAIN STEAM BREAK

PLOT-1 : FROM WE WPT-G987 & WPT GGG8
PLOT-2 : FROM MECH. CALC. 511-12B, REV.0
PLOT-3 : FROM MECH. CALC. 511-12B, REV.0

APPENDIX I
FIGURE-2

APPENDIX II
FIGURE 1

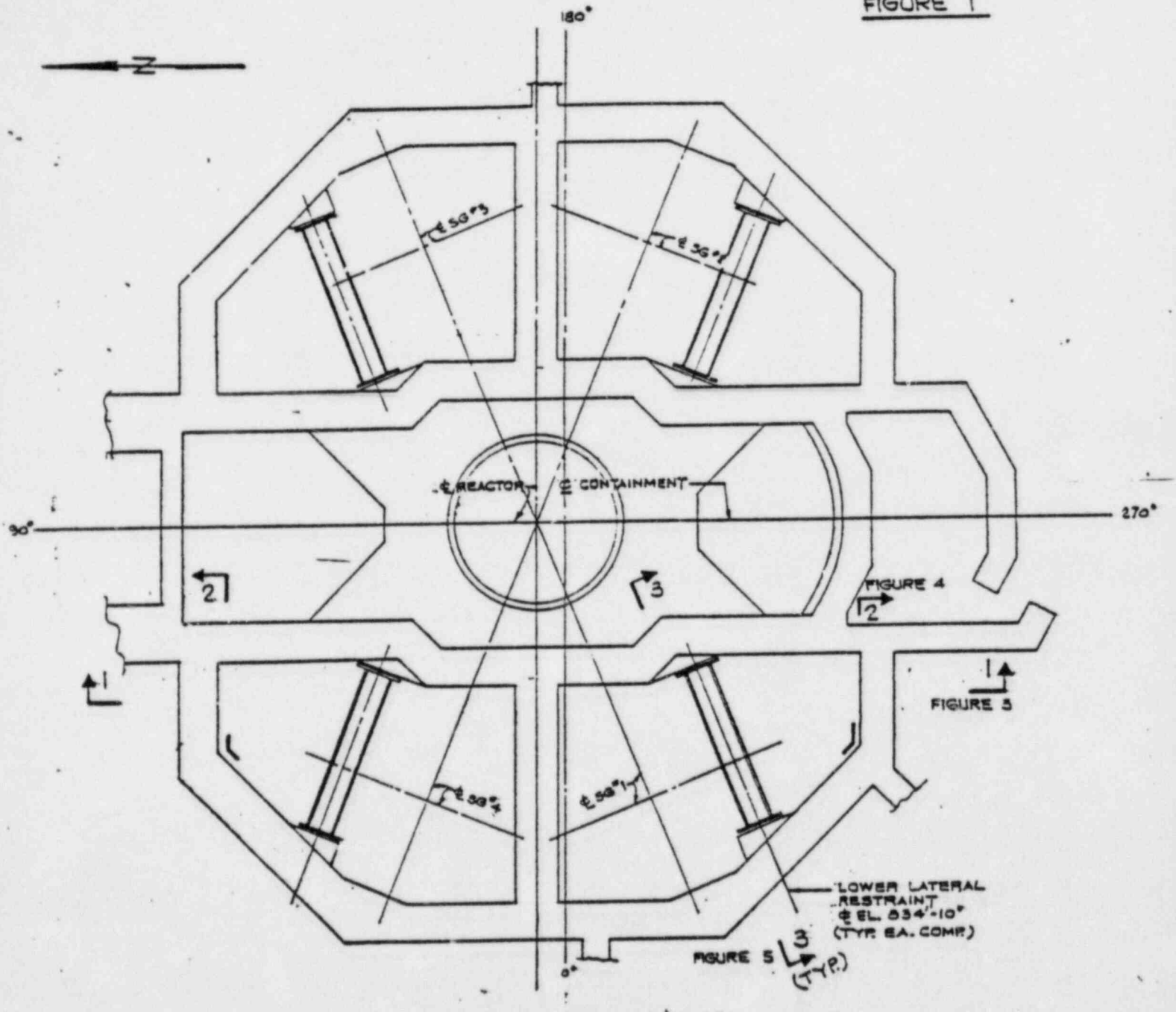

PLAN AT EL. 834'-10"
- S. G. COMPARTMENTS

4-13-84

APPENDIX II
FIGURE -2

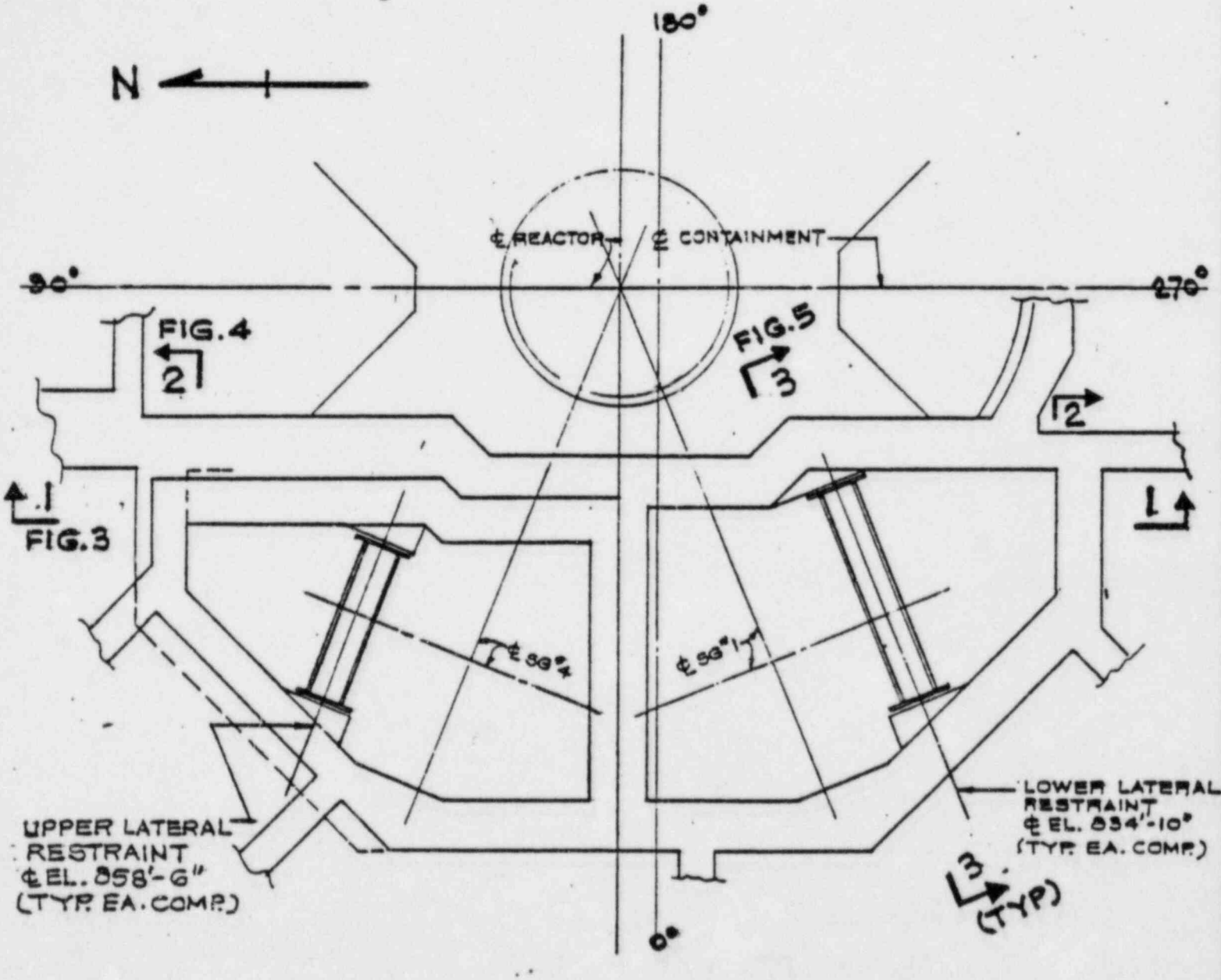

PLAN - S.G. COMPARTMENTS
(WALLS USED IN THE MODEL)

APPENDIX II
FIGURE 3

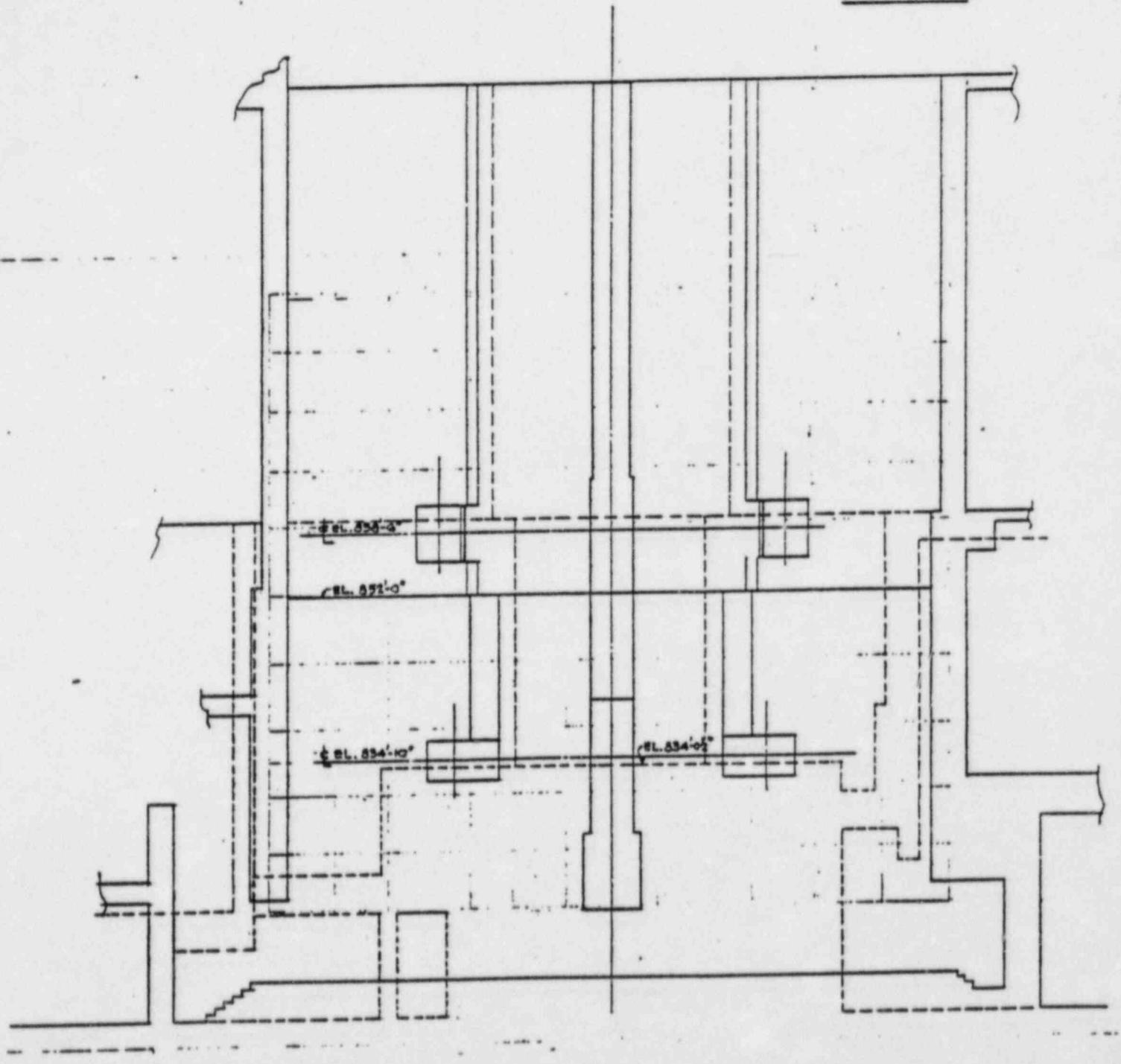

SECT. 1-1

APPENDIX II
FIGURE 4

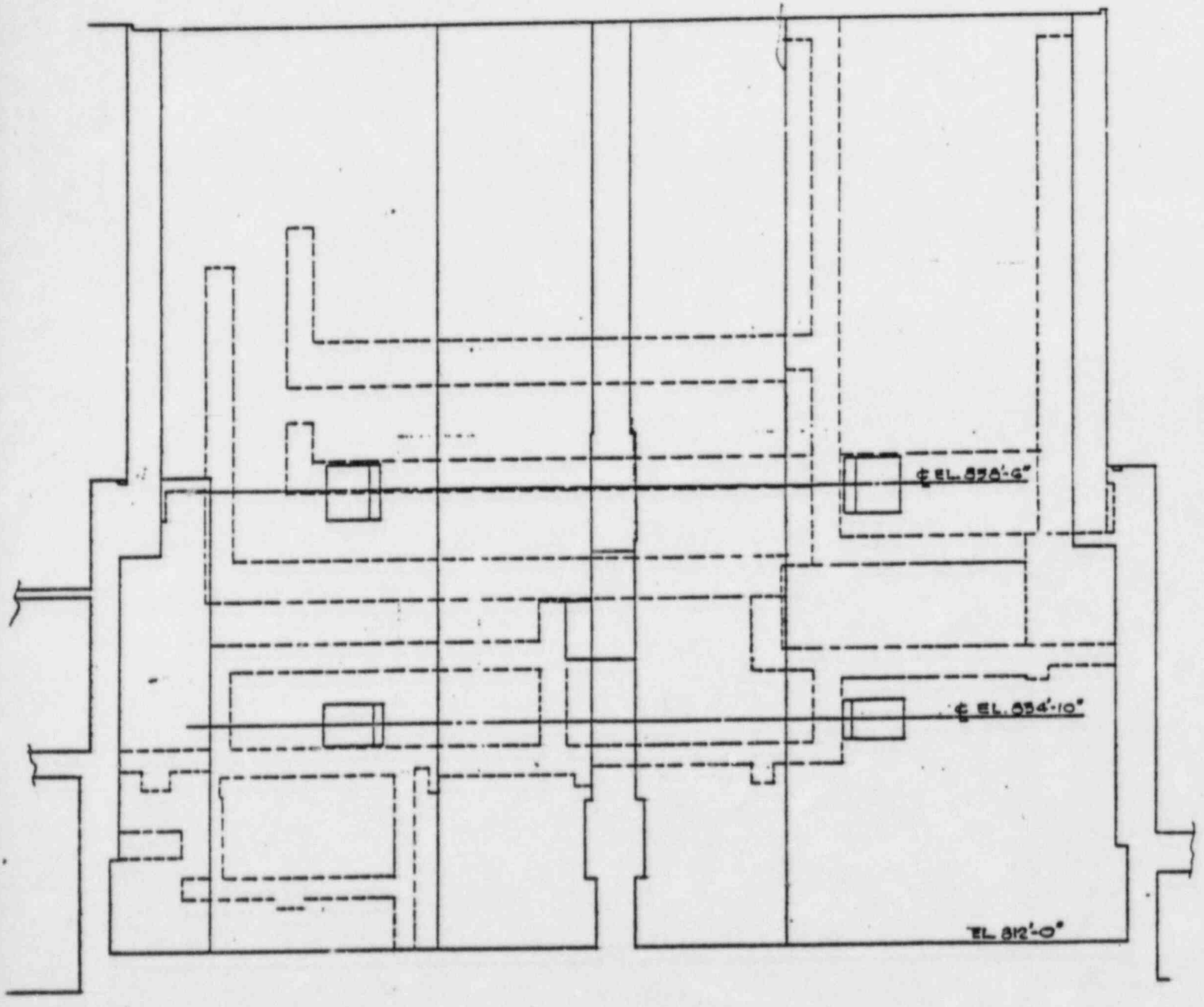

SECT. 2-2

APPENDIX II
FIGURE 5

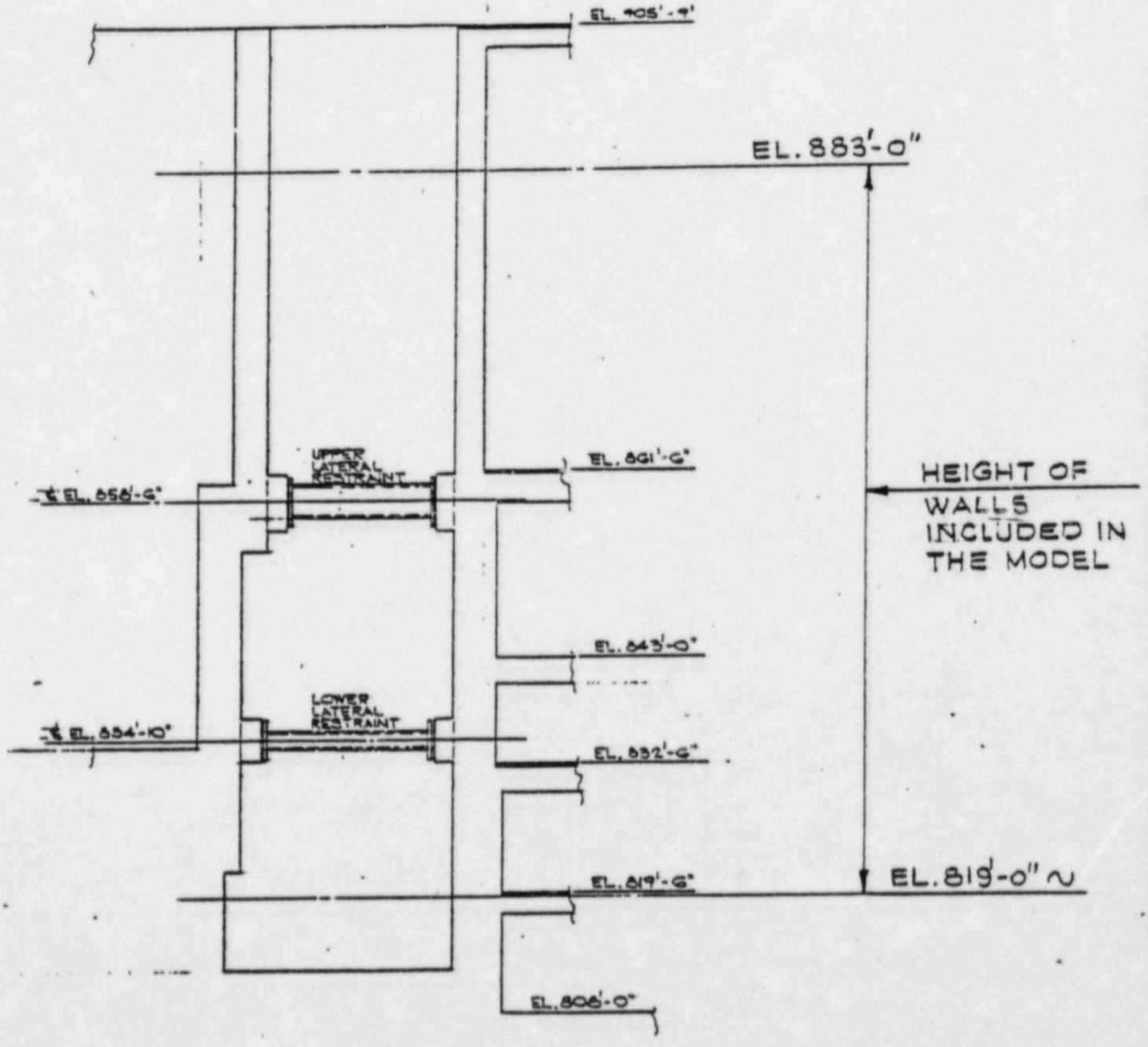

SECT. 3-3

NONLINEAR ANALYSIS OF RC STRUCTURE WITH INTERACTION OF THERMAL CRACKING AND MECHANICAL LOAD

H-S CHANG, R ATKATSH
Ebasco Services, Inc, Two Rector Street, New York, NY 10006, USA

D N HERTING
Universal Analytic, Inc, 7740 West Manchester Blvd, Playa Del, CA 90291 USA

SUMMARY

In recent years, finite element methods became a major tool in the analyses of reactor concrete containment and drywell structure of BWR type containment. In these analyses, linear elastic method is acceptable for mechanical loads because the cracking of the concrete will not alter appreciably the stress distribution in the structure. However, it breaks down completely with the interaction of mechanical loads and high thermal loads, which is characteristic of containment structure. Usual practice is to adjust either the material property of the concrete before the analysis or the solution after the analysis. Complicated geometrical configuration and thermal distribution make this kind of adjustments not only difficult, but its outcome unpredictable.

A series of flat shell elements with coupled in-plane stiffness and off-plane stiffness are formulated by using Kirchoff's assumptions. These elements are divided into layers along the thickness, and each layer can have its own material characteristics. The crackings of the concrete are propagating from layer to layer and from element to element. At each stage, the equivalent thermal load vector corresponding to the current material state are evaluated and combined with external mechanical load. The nonlinear solution method used is a combination of so called variable stiffness method and initial strain method. This series of elements and nonlinear solution methods are implemented into the NASTRAN (NASA Structural Analysis) computer program. Material assumptions, formulation of the elements, criteria to establish crack opening and closing, methods to construct the thermal load and nonlinear load, methods to handle the interaction of thermal load and mechanical load, nonlinear iteration scheme and solution convergence criteria, and computer program configuration are discussed in the paper. Also examples to compare with experimental data and application to the analysis are presented in the paper. A nonlinear finite element method is derived and implemented to solve the problem of interaction of thermal cracking and mechanical load in reinforced concrete structure. The algorithm is designed to be efficient for the solution of large-order and complex structure, such as reactor containment, and eliminate the uncertainty in handling the thermal load. Its results show that it can predict cracking propagation and stress redistribution in reasonable agreement with available experimental data.

1. Introduction

In recent years, the finite element method became a major tool in the analysis reactor concrete containment and drywell structure of DWR type containment. In these analyses, the reinforced concrete is usually assumed to be linear elastic and homogeneous. The stresses distribution characteristics, such as off-plane shear, in-plane forces, bending moment and twist, are obtained from these analyses. Then, locally, the reinforced concrete is designed as structural members by following long established semi-empirical design method. Under external mechanical load, such as pressure and seismic load, this procedure is acceptable becasue the cracking of the concrete will not alter appreciably the stress distribution in the concrete. However, it breaks down completely under the interaction of the thermal and the mechanical load, because the magnitude of the thermal stresses depend on the material of the concrete (cracking), which in turn depends on the stress state in the concrete. Thus, they couple each other nonlinearly. Therefore, the stress characteristics obtained from a linear elastic analysis does not represent the real stress distribution under the interaction of the thermal and the mechanical load. To remedy this, the usual practice is to adjust either the material property of the concrete before the analysis, or adjust the solution after the analysis. However, for structures with complicated geometrical configuration and complicated thermal distribution, this kind of adjustment is not only difficult, but its outcome unpredictable.

From the above discussion, the analysis method for the reinforced concrete structures under the interaction of the thermal load and the mechanical load needs improvement. In the past few years, the nonlinear analysis of the concrete structures gradually gain acceptance [1, 4, 5]. In these nonlinear analyses, the material property of the concrete at each stage of loading can be accurately predicted; and, thus, the thermal load can be evaluated properly. Furthermore, the advancement of high-speed computer and matrix manipulation software make a nonlinear solution of a large order structure model possible. In view of the strigent safety requirements of containment structure and the uncertainty of existing analysis methods in dealing with the thermal load, a nonlinear analysis for the interaction of thermal load and the mechanical load seems to be the answer.

In order to handle large-order and complex structural models, not only a valid nonlinear analysis procedure but also a large versatile finite element computer code is needed. To accomplish this, a series of flate layered shell elements and a nonlinear analysis procedure are implemented into the computer

code NASTRAN (NASA Structure Analysis) Level 16. The new elements are compatible with all other elements in the NASTRAN family. Input data reduction and matrix manipulation are done by standard NASTRAN. Special consideration has been taken to design the nonlinear analysis algorithm so that it is efficient for the solution of large-order and complex structural models.

2. Layered Shell Element

In general, the stiffness matrix of a shell element can be expressed as

$$[K_{ee}] = \int_A [B]^T [D][B] \, dA \tag{1}$$

where $[B]$ is the strain-displacement relation matrix and $[D]$ is the generalized stress-strain relation matrix. The $[B]$ matrix is a function of the geometrical shape of the element and the assumed displacement shape function. In this work, three new flat shell elements have been implemented into NASTRAN. The formulation of the $[B]$ matrices of these three elements followed those of NASTRAN TRBSC, TRIA1 and QUAD1 elements [7]. In NASTRAN, the in-plane and off-plane stiffnesses are computed independently. However, for the new elements, the in-plane stiffness and off-plane stiffness are coupled. Especially, for TRIA1 element, which is a Clough triangle; the Clough's method of constraint is extended to include the coupling of the in-plane and the off-plane terms.

The $[D]$ matrix is a function of the material property of the element only. In evaluation of the $[D]$ matrix, the concept of layer finite elements are adopted in this work. A typical layered element is shown in Figure 1. Each layer of the element is corresponding to a unique material property which may be defined independently or changed to a new material property as the nonlinear analysis progresses. Although the stress may be different from one point to another in the plane of each layer, it is assumed to be constant throughout the thickness of the layer. For nonlinear material, the material property of a layer is assumed to be a function of the average stress in that layer.

For material nonlinearity, the $[B]$ matrix is independent of the nonlinear behavior of the element. In order for efficient execution of larger order structural model, the $[B]$ material is computed outside of the nonlinear iteration loops and stored on a random file, which will be read back to generate the stiffness matrix, equivalent thermal load, and unbalanced load vector.

3. Material Property and Constitutive Relations

Concrete is considered to be a linear elastic-brittle material with a limited tensile strength f_t. The reinforcing steel is considered linear elastic. The failure criterion for concrete under bi-axial stress state is shown in Figure 2. The dotted line is proposed by Kupper, Hilsdorf and

Rush [3], and the solid line is used in this analysis. The concrete is considered cracked in Regions I, II and III. Since the material property of a layered element may be different from one layer to another, each layer has its own stress strain relations. These relations can be expressed as

$$\{\sigma\} = [C]\{\epsilon\} \tag{2}$$

where $\{\sigma\} = \{\sigma_x, \sigma_y, \tau\}^T$ is a layer stress vector and $\{\epsilon\} = \{\epsilon_x, \epsilon_y, \gamma\}^T$ is a layer strain vector. Before cracking, the concrete is considered to be homogeneous and isotropic, the $[C]$ matrix is the usual isotropic elasticity matrix. For concrete with one crack, the $[C]$ matrix is

$$[C] = [T(\theta)]^T \begin{bmatrix} 0 & 0 & 0 \\ 0 & E_c & 0 \\ 0 & 0 & \beta G_c \end{bmatrix} [T(\theta)] \tag{3}$$

where E_c is the Young's modulus for concrete and G_c is the shear modulus. β is a shear retention coefficient accounted for aggregate interlocking effect of concrete [1]. $[T(\theta)]$ is a transformation matrix from the coordinate system normal to the crack to the element coordinate system (Figure 3). For concrete with two cracks, in Region III of Figure 2, the $[C]$ is assumed to be identically zero. For reinforcement, the $[C]$ matrix is

$$[C] = [T(\theta)]^T \begin{bmatrix} E_s & 0 & 0 \\ 0 & 0 & 0 \\ 0 & 0 & 0 \end{bmatrix} [T(\theta)] \tag{4}$$

where E_s is the Young's modulus for steel and $[T(\theta)]$ is the transformation matrix from the coordinate system tangential to the reinforcing bar to the element coordinate.

As defined in Eq (1), the element internal force vector is related to the generalized strain vector by the $[D]$ matrix,

$$\{F\} = [D]\{\lambda\} \tag{5}$$

where $\{F\} = \{F_x, F_y, F_{xy}, M_x, M_y, M_{xy}\}^T$, F_x, F_y, F_z are membrane forces and M_x, M_y, M_{xy} are moments, $\{\lambda\} = \{\epsilon_{ox}, \epsilon_{oy}, \gamma_o, \chi_x, \chi_y, \chi_{xy}\}^T$, ϵ_{ox}, ϵ_{oy}, γ_o are strains at mid-surface of the element. In order to relate the layer strain vector $\{\epsilon\}$ and the element strain vector $\{\lambda\}$, the Kirchoff assumptions are used. The Kirchoff assumption can be expressed by

$$\{\sigma\} = [H]\{\lambda\} \tag{6}$$

$$[H] = \begin{bmatrix} 1 & 0 & 0 & -z & 0 & 0 \\ 0 & 1 & 0 & 0 & -z & 0 \\ 0 & 0 & 1 & 0 & 0 & -z \end{bmatrix}$$

where z is the location at which the strain vector $\{\epsilon\}$ is evaluated. Now, the $[D]$ matrix can be evaluated by the equation,

$$[D] = \int_z [H]^T [C][H] \, dz \tag{7}$$

4. Changing of Material State

Since the material state of a concrete layer is a function of the stresses and strains in that layer, it will change from one state to another as the nonlinear analysis progresses. There are three major modes of changing state:

1) the formation of a new crack;

2) the closing of an existing crack;

3) the reopening of a closed crack.

Mode (1) is the only mode dealt by most investigators [1, 4, 5], and it is applicable to a monotonically increasing loading. Mode (2) is essential if it is to investigate the structural behavior including the interaction of the thermal load and the mechanical load. In order to reduce the amount of book-keeping, it is assumed that mode (3) is identical to mode (1) in this work. This assumption is true if the tensile strength of concrete is zero. In view that the tensile strength of concrete is small and that it is often neglected in most engineering analyses because of its uncertainty, this assumption is a good approximation.

The criteria for the formation of new crack is based on the layer stresses: a layer will crack if the computed principal tensile stress exceeds the tensile strength of the concrete specified in Figure 2, i.e.

$$\sigma_t \geq f_t^1 \tag{8}$$

where σ_t is the average principle stress of the layer and f_t^1 is defined by the solid line in Figure 2. The normal of the crack is assumed to be in the principal tensile direction. The criteria for the closing of an existing crack is based on the layer strains: an existing crack will close if the average layer strain normal to the existing crack becomes equal or less than zero, i.e.,

$$\begin{aligned} \epsilon_n + \mu \epsilon_t \leq 0 \quad &\text{if} \quad \epsilon_t < f_t^1 / E_c \\ \epsilon_n \leq 0 \quad &\text{if} \quad \epsilon_t \geq f_t^1 / E_c \end{aligned} \tag{9}$$

where ϵ_t is the strain tangential to the existing crack and μ is the Poisson ratio. The procedure to evaluate the changing of material state for each layer is proceeded as follows:

a) Compute the layer strains by

$$\{\epsilon\} = [H][B]\{u\} - \{\alpha\}T \tag{10}$$

where $\{u\}$ is the displacement solution vector of the current iteration for the current element, $\{\alpha\}$, the thermal expansion coefficient vector and T, the Layer temperature.

b) If the layer has existing cracks, the computed strains are tested against Eq (9) to form an intermediate new Layer stress-strain relation $[C_1]$, i.e.,

$$[C_o] \xrightarrow{\text{existing cracks closing?}} [C_1] \tag{11}$$

where C_o is the current Layer stress-strain relations built into the global stiffness matrix, which is used to obtain the displacement solution vector $\{u\}$.

c) If no existing crack in the layer, let $[C_1] = [C_o]$.

d) Based on the new layer stress-strain relation $[C_1]$, the layer stresses are computed and tested against the criteria specified by Eq (8) to form the final new layer stress-strain relation $[C_2]$

$$[C_1] \xrightarrow{\text{new cracks forming?}} [C_2] \tag{12}$$

5. Equivalent Thermal Load Vector

The equivalent thermal load vector is dependent on the material property of the element. With the new material property defined by the $[C_2]$ matrix of Eq (12), the equivalent thermal load vector for the new material is evaluated by

$$\{f_t\} = \int_A [B]^T \int [K]^T [C_2] \{\alpha\} \; T(z)\, dz\, dA \tag{13}$$

6. Nonlinear Solution Method

Generally, two iteration methods are available in the finite element method for the solution of material nonlinear problems: the so-called variable stiffness method and the initial stress/strain method [9]. For variable stiffness method, a solution is first obtained by the initial linear system. Based on this solution, the material state of each element is updated, and a new solution is obtained with the regional load vector and the new material state. This process continues until the change of material state of two consecutive states are sufficiently small. For the initial stress/strain method, the original elastic system stiffness is kept unaltered. At each iteration, the difference between the element stresses which are consistent with the current material state and the element stresses which are in equilibrium with the external loads are called the unbalanced stresses. From these unbalanced stresses, the equivalent unbalanced load vectors are

found. Then, a new solution is obtained with these additional unbalanced load vectors and the original linear system stiffness matrix. This process continues until the change of unbalanced vector is negligible. The variable stiffness method has the deficiency of reassembling system stiffness at every iteration. This process is expensive. On the other hand, the initial stress/strain method has the deficiency of slow convergence. In this work, a combination of both methods are used, and the iteration equation can be expressed as

$$\left[K_o\right]\left\{u^{j+1}\right\} = \left\{f_a\right\} + \left\{f_t^j\right\} + \left\{f_u^j\right\} \tag{14}$$

where $\left[K_o\right]$ is the updated system stiffness matrix, $\left\{f_a^j\right\}$ is the external load vector, $\left\{f_t^j\right\}$ is the thermal load vector based on the current material state and $\left\{f_u^j\right\}$, the unbalanced load vector given by

$$\left\{f_u^j\right\} = \left(\int_A \left[B\right]^T \int_z \left[H\right]^T \left[C_2\right] - \left[C_o\right]\left[H\right] dz \left[B\right] dA \right) \left\{u^j\right\} \tag{15}$$

where $\left[C_2\right]$ and $\left[C_o\right]$ are the stress/strain relation for the new material state (Eq (12)) and the state built into the current system stiffness matrix $\left[K_o\right]$, respectively. The convergence criterion adopted are given by

$$\left| \frac{\left\{f^j - f^{j-1}\right\}^T \left\{u^j\right\}}{\left\{f^j\right\}^T \left\{u^j\right\}} \right| < \delta$$

where $\left\{f^j\right\}$ is total load vector on right-hand side of Eq (14) and δ is a sufficiently small number.

7. NASTRAN Implementation

The implementation of the cracking analysis algorithm in NASTRAN requires only isolated interfaces to the program due to NASTRAN's modular design. Most of the new solution iteration procedure code are isolated to five new modules, which uses many of the existing NASTRAN matrix subroutines. A brief description of each module appears below:

a) Function Module CASMG (Strain Matrix Generator)

Generates the element stress-strain relations $\left[B\right]$. This module is outside the iteration loops and store the $\left[B\right]$ matrix on random access files called CACF (Cracking Analysis Operation File). These data will be used inside the iteration loops to compute thermal load, element stresses and unbalanced load vectors.

b) Function Module CAUTIL (Cracking Analysis Utilities)

Performs utility function such as extracting data from CACF for previous material states and assembling portion vectors for module CAITER (described below).

c) Function Module CAEMG (Element Stiffness Generator)

Generates the new element stiffness matrices.

d) Functional Module CAITER (Crack Analysis Iteration)

Generates the nonlinear thermal load vector and the unbalanced load vector and performs the unbalanced load iteration.

e) Function Module CAOUTP (Cracking Analysis Output Processor)

There are two iteration loops; the outer loop is called the stiffness iteration which updates the system stiffness on the left-hand side of Eq (14); the inner loop is called unbalanced load iteration which iterates the right-hand side of Eq (14) with constant $[K_o]$. The stiffness iteration is implemented by using the NASTRAN DMAP (Direct Matrix Abstraction) control language [8]. Module CAITER performs the unbalanced load iteration. It recovers the stresses, evaluates nonlinear material state, generates thermal load vector and unbalanced load vector, tests for convergence, and setting of parameters to control DMAP execution. The CASMG module resides outside both iteration loops.

8. Example Problems

a) McNeice's Plate

The McNeice's plate [2] is a 36 inch square by 2 inch thick supported at four corners. It is a two-way slab with 0.85% reinforcing bars. A concentrate force is acting at the center of the plate. Figure 4 shows the finite element grid and the load deflection curves from experimental and computed results for point 2 on the plate.

b) Infinite Long Cylindrical Shell Under Thermal Load

Figure 4 shows a cylindrical shell of 15 feet inside radius and 1 foot thickness with two-way reinforcing bar at outside face of the cylinder. It has a as built temperature of 50° F. This temperature grows to 170° F outside of the cylinder and 80° F inside of the cylinder. The results of classical theory and this analysis are shown in Figure 4. The small discrepancy in cracking distance and the amount of increasing in radius is due to the assumption that stresses are constant throughout the thickness of a layer.

References

1 HAND, F.R., PECKNOLD, D.A., SCHNOBRICH, W.C., "Nonlinear Layered Analysis of RC Plates and Shells," JOURNAL OF THE STRUCTURAL DIVISION, July, 1973.

2 JOFRIET, J.C., McNEICE, G.M., "Finite Element Analysis of Reinforced Concrete Slabs," JOURNAL OF THE STRUCTURAL DIVISION, ASCE, Volume 97, No. ST3, Proc. Paper 7963, March, 1971, pp 785-806.

3. KUPFER, H., HILSDORF, H.K., RUSCH, H., "Behavior of Concrete Under Biaxial Stresses," JOURNAL OF THE AMERICAN CONCRETE INSTITUTE, Volume 66, No. 8, August, 1969, pp 656-666.

4. VALLIAPPAN, S., DOOLAN, T.F., "Nonlinear Stress Analysis of Reinforced Concrete," JOURNAL OF THE STRUCTURAL DIVISION, ASCE, Volume 98, ST4, Proc. Paper 8845, April, 1972, pp 885-898.

5 PHILLIPS, D.V., ZIENKIEWICZ, O.C., "Finite Element Nonlinear Analysis of Concrete Structures," Proc. Instn. Civil Engineers, Part 2, 1976, 21, March, 59-88.

6 HERTING, D., HERENDEEN, D., HOESLEY, R., CHANG, H., "Implementation on a Nonlinear Concrete Cracking Algorithm in NASTRAN," Fifth NASTRAN User's Colloquium, Amers Research Center, October 5-6, 1976.

7 NASA SP-221(03), "The NASTRAN Theoretical Manual Level 16.0."

8 NASA SP-222(03), "The NASTRAN User's Manual Level 16.0."

9 ZIENKIEWICZ, O.C., "The Finite Element Method in Engineering Science," McGraw-Hill, London, 1971.

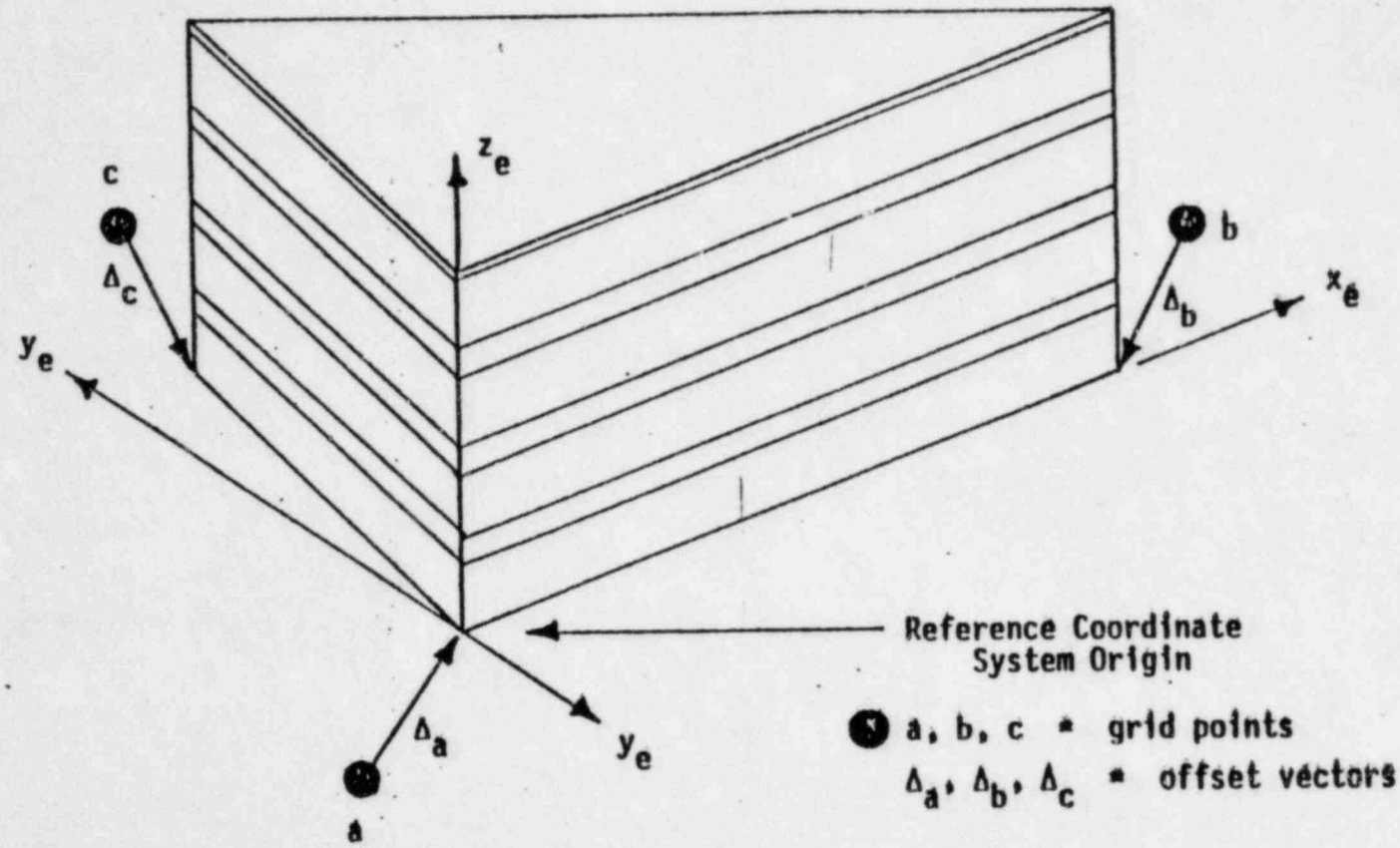

FIGURE 1. TRIANGULAR LAYERED ELEMENT

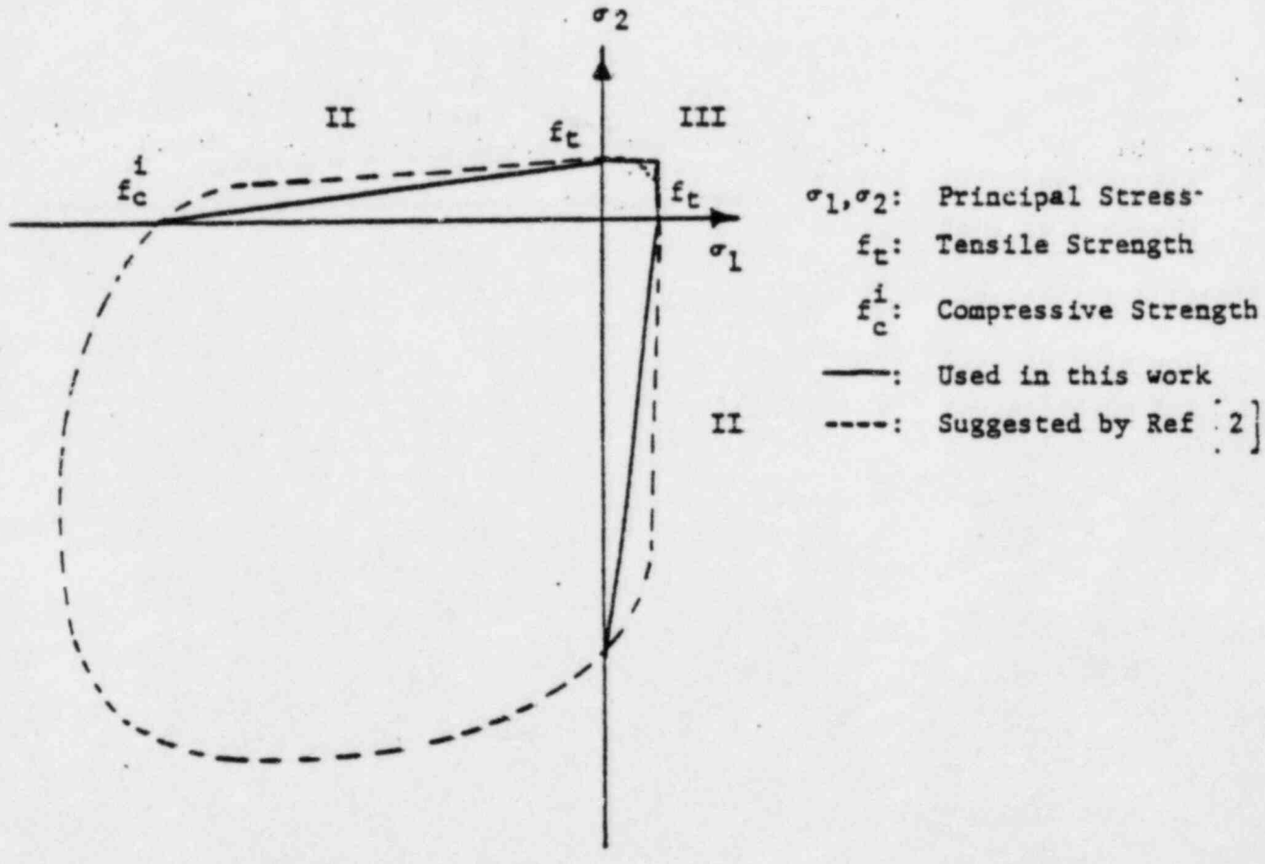

FIGURE 2. CONCRETE FAILURE CRITERIA UNDER BIAXIAL STRESSES

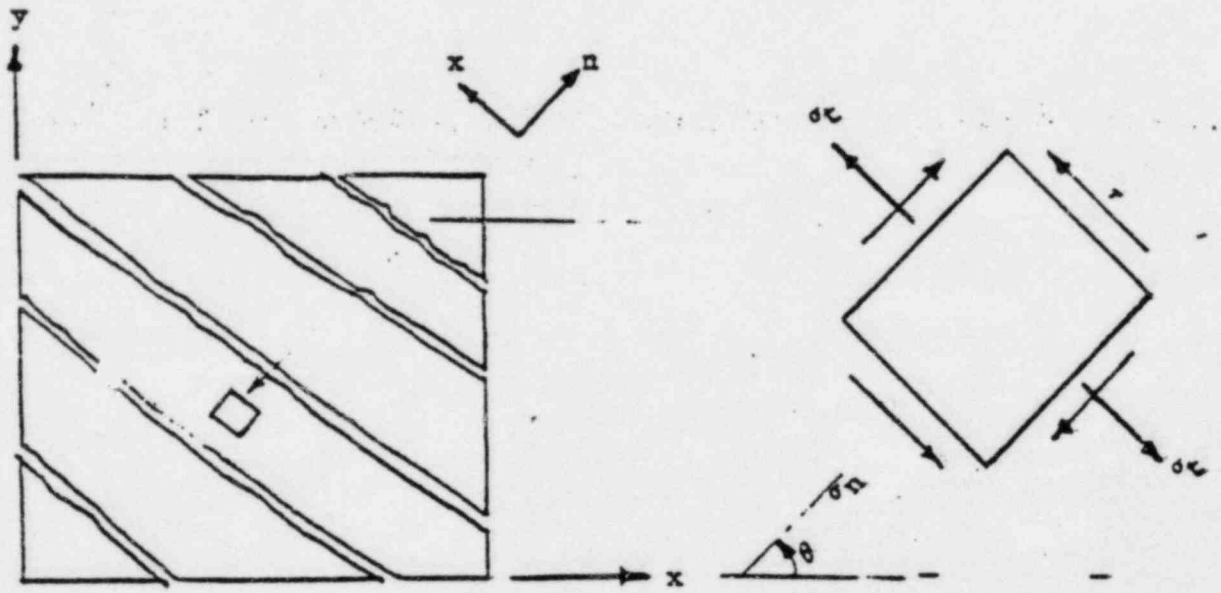

FIGURE 3. LAYER STRESSES IN CONCRETE WITH ONE CRACK

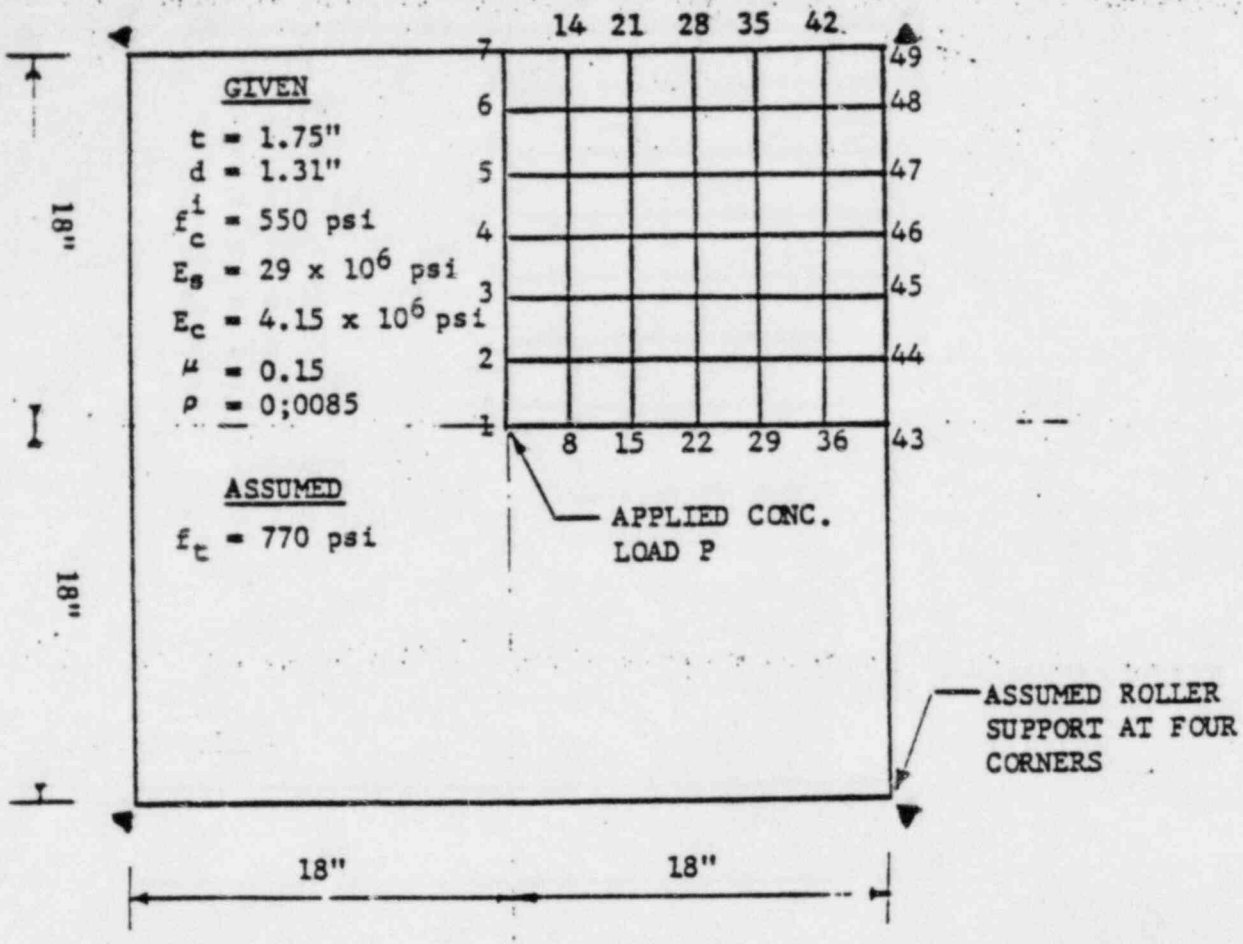

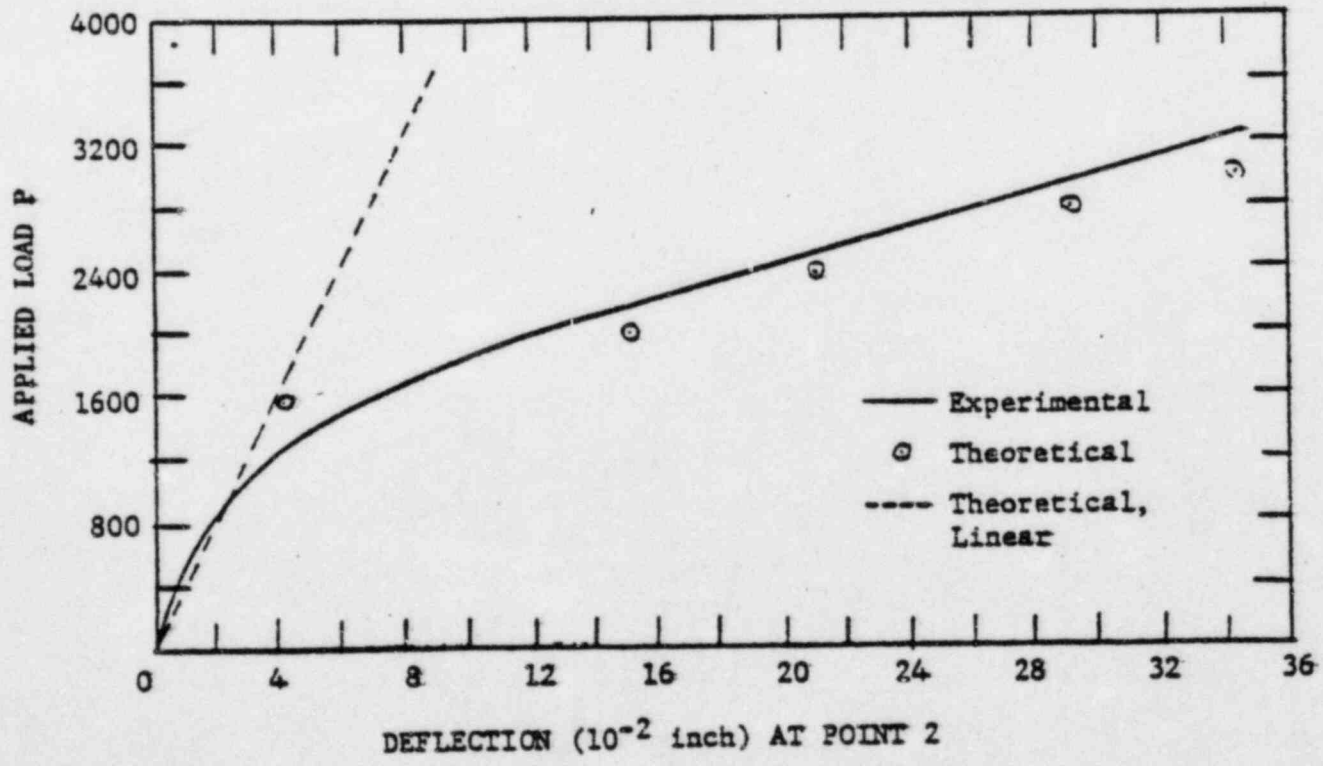

FIGURE 4. McNEICE'S PLATE

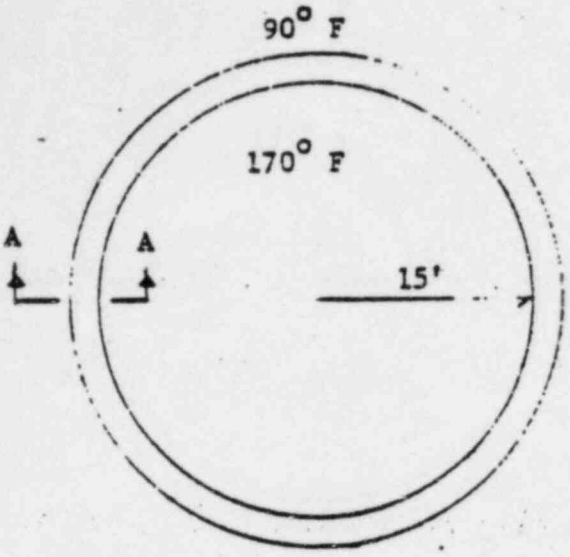

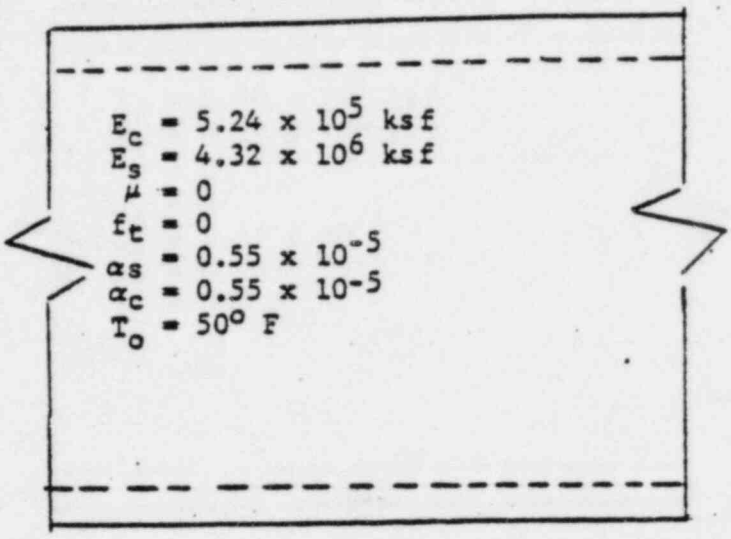

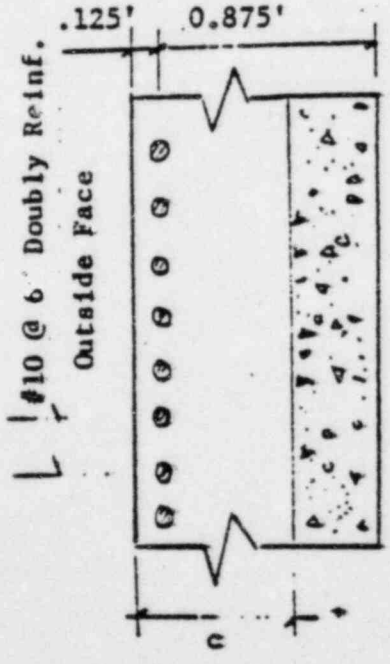

CRACKED ZONE

SECT. A-A

	THIS ANALYSIS	CLASSICAL THEORY
Growth of Radius	7.31×10^{-3} ft	7.49×10^{-3} ft
Stress in Reif. Bar	1058 psf	1059 psf
Max Stress in Concrete	98.4 psf	98.4 psf
Cracking Distance C	0.6 ft	0.621 ft

FIGURE 5. INFINITE CYLINDRICAL SHELL UNDER THERMAL LOAD

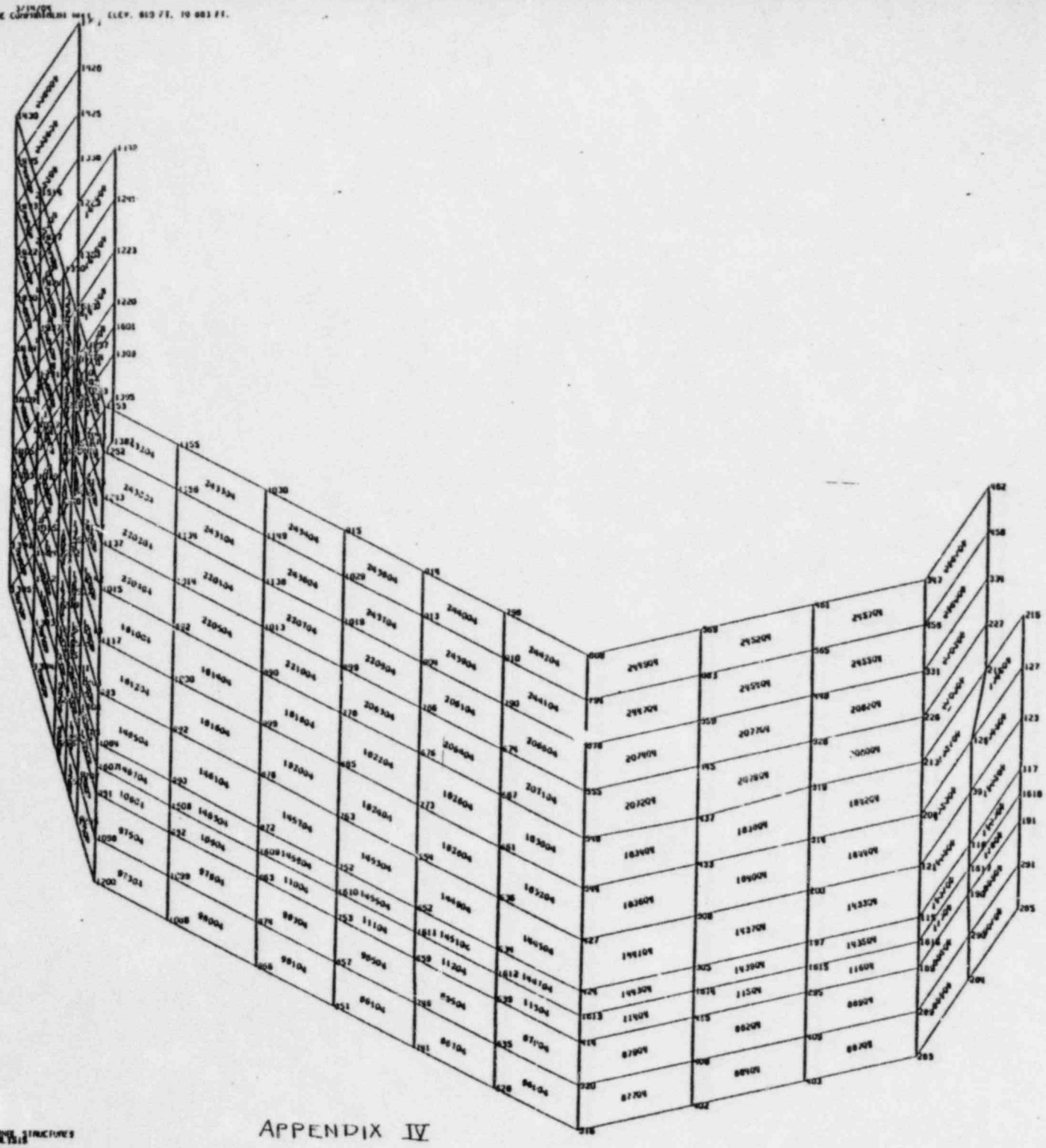

APPENDIX IV

FIG. 1

BACK OF COMPARTMENT WALL ELEV. 819 FT. TO 863 FT.

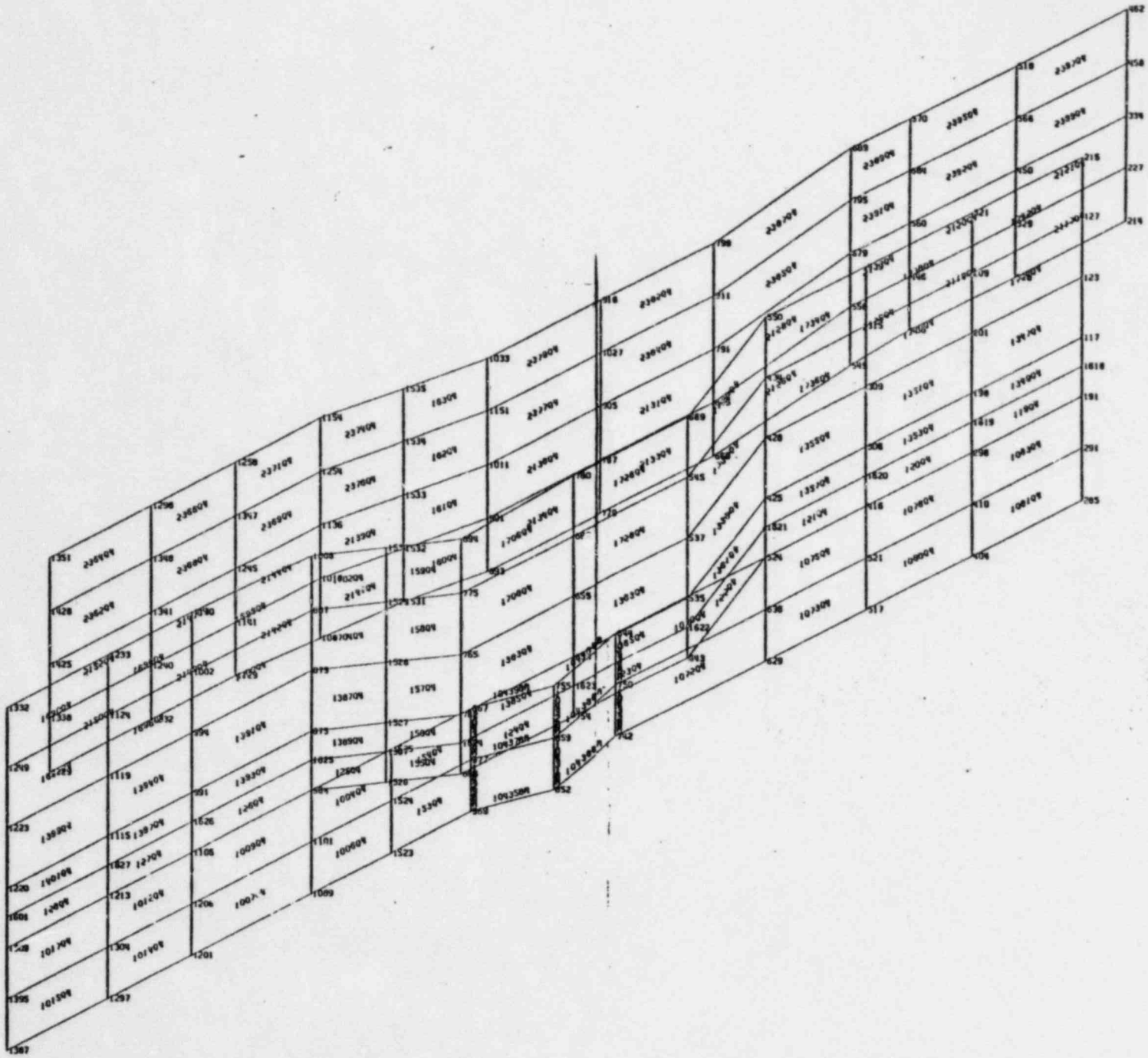

APPENDIX IV

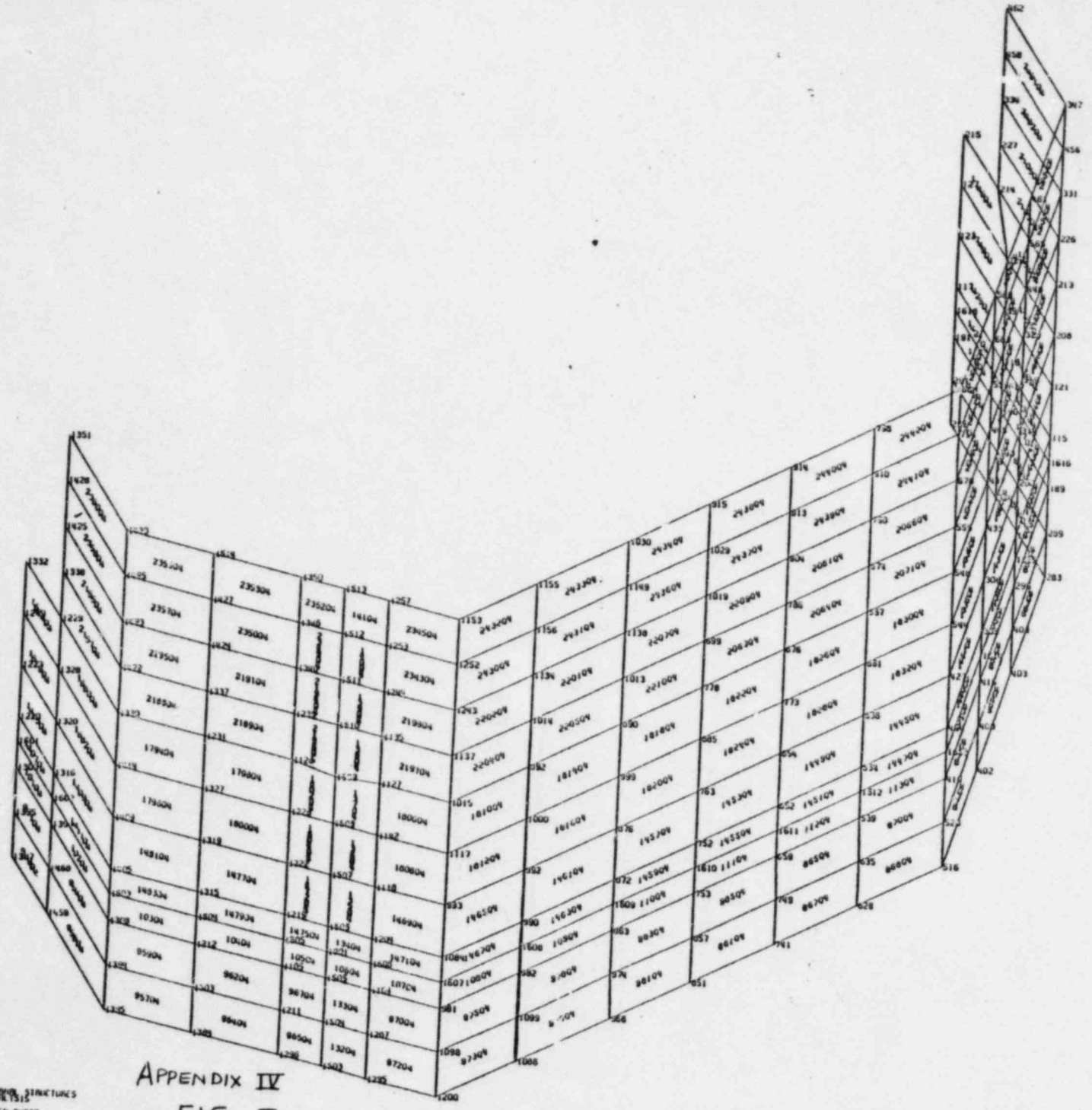

APPENDIX IV

FIG. 3

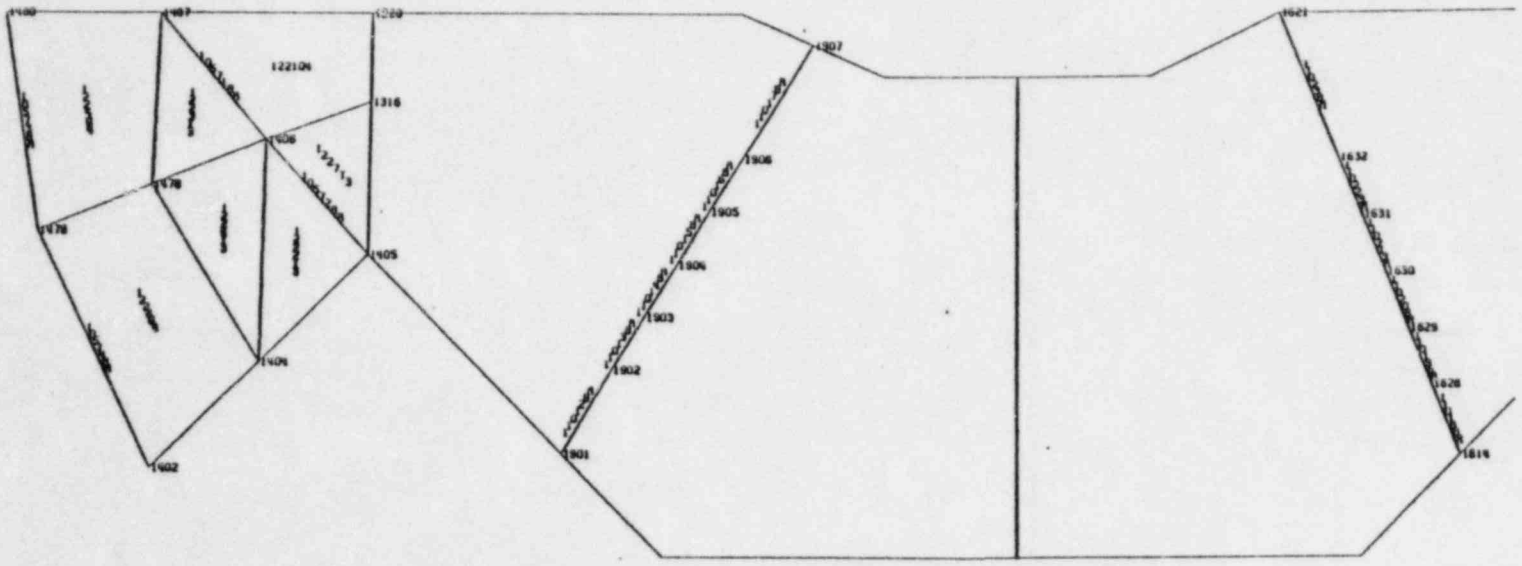

APPENDIX IV

FIG. 4

1

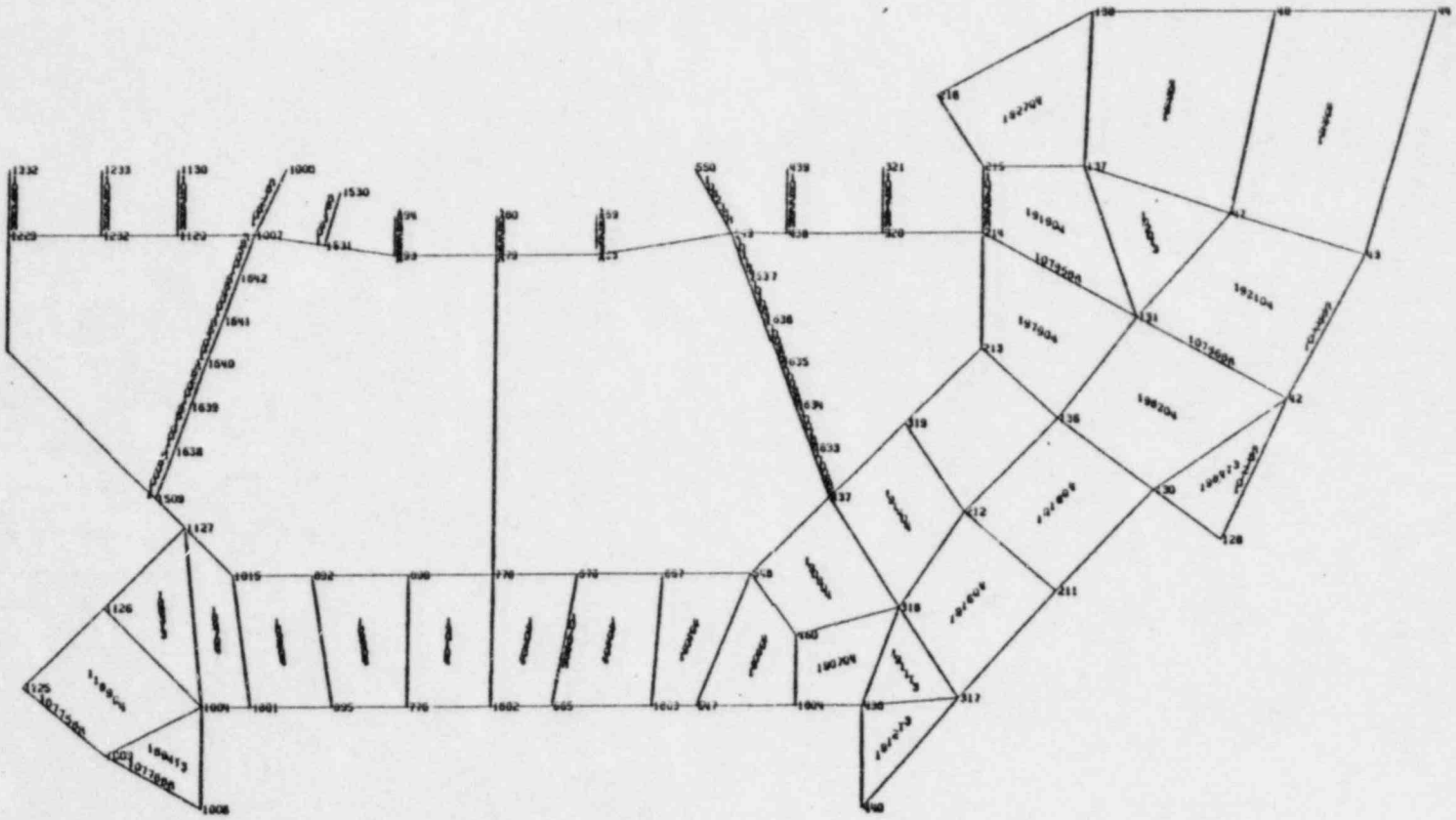

APPENDIX IV

FIG. 5

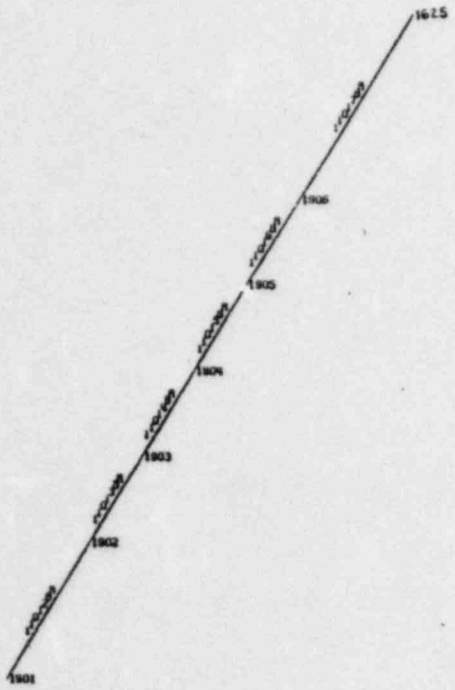

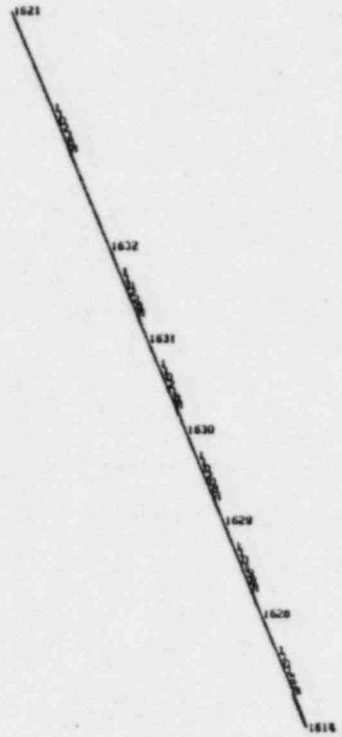

APPENDIX IV

FIG. 6

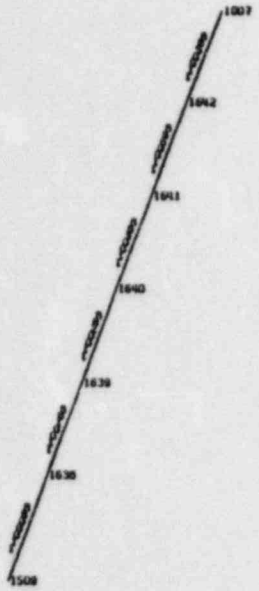

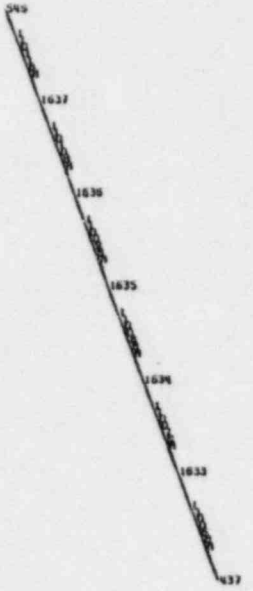

APPENDIX IV
FIG. 7

UNDEFORMED SHAPE

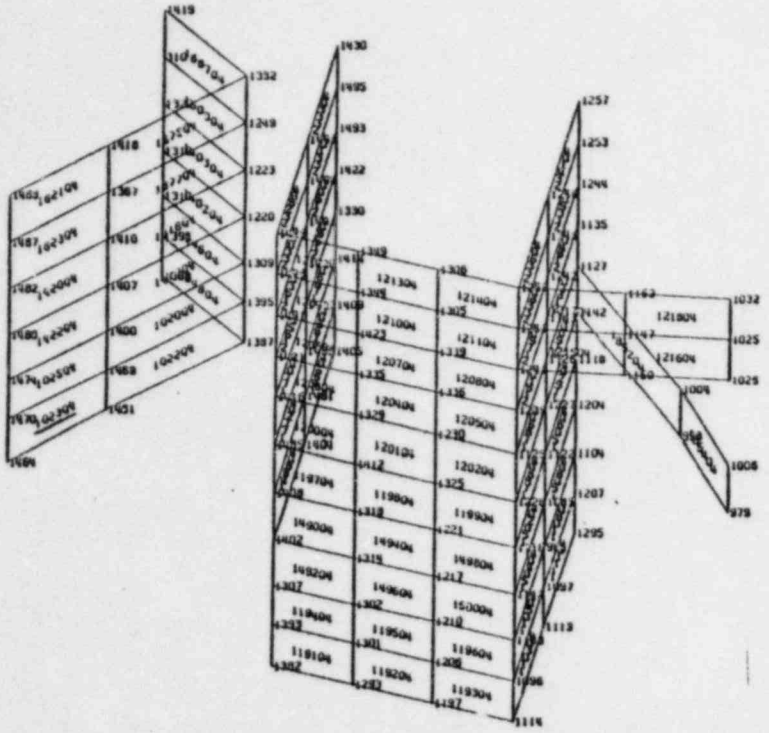

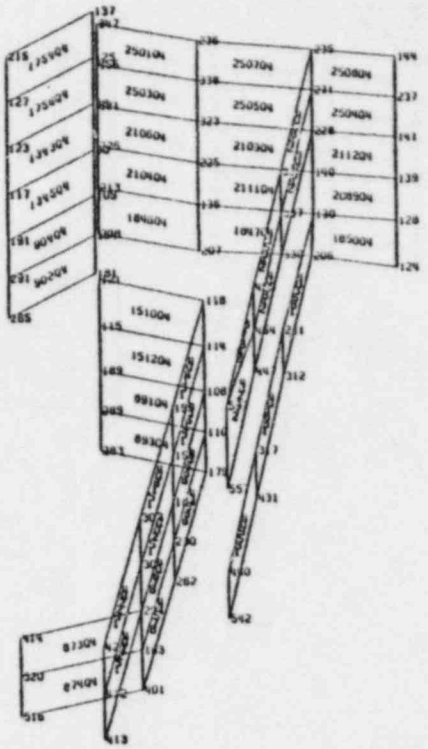

APPENDIX IV

FIG. 8

UNDEFORMED SHAPE

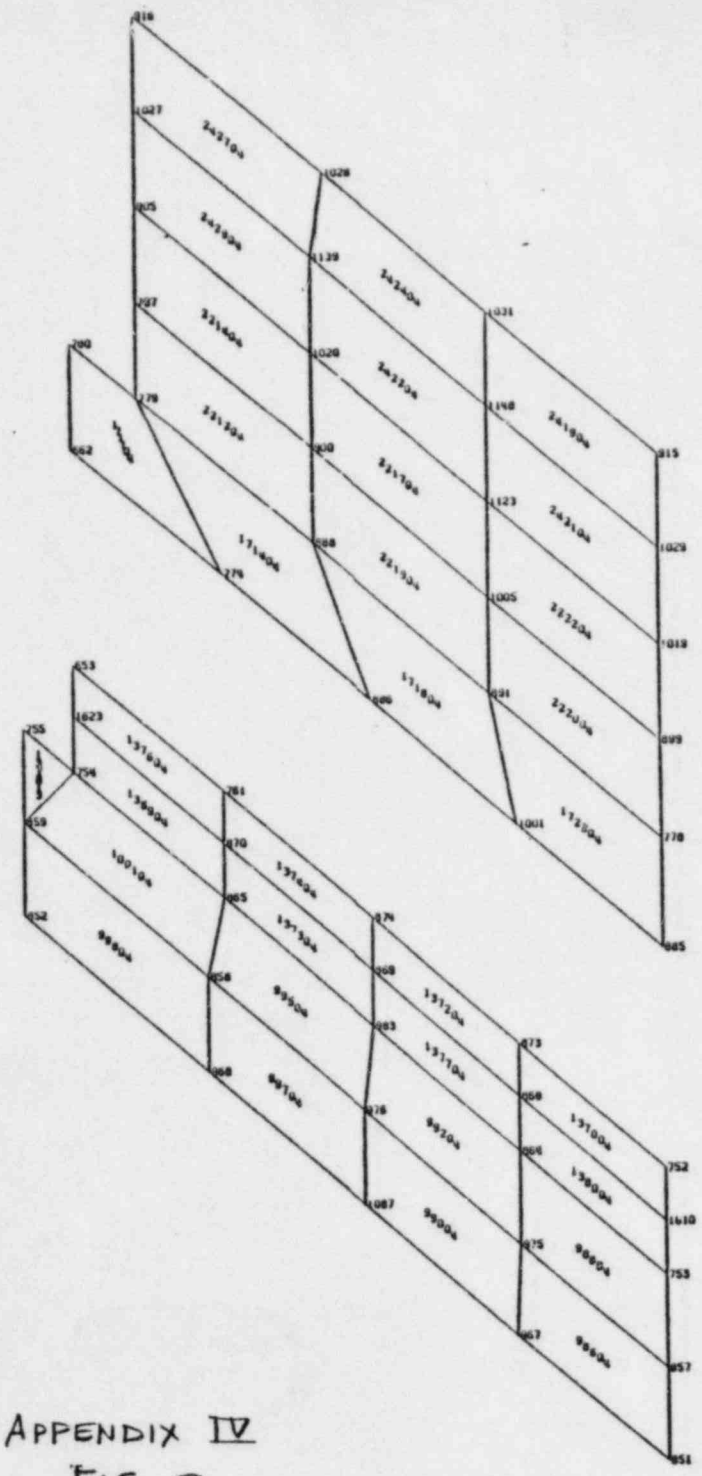

APPENDIX IV

FIG. 9

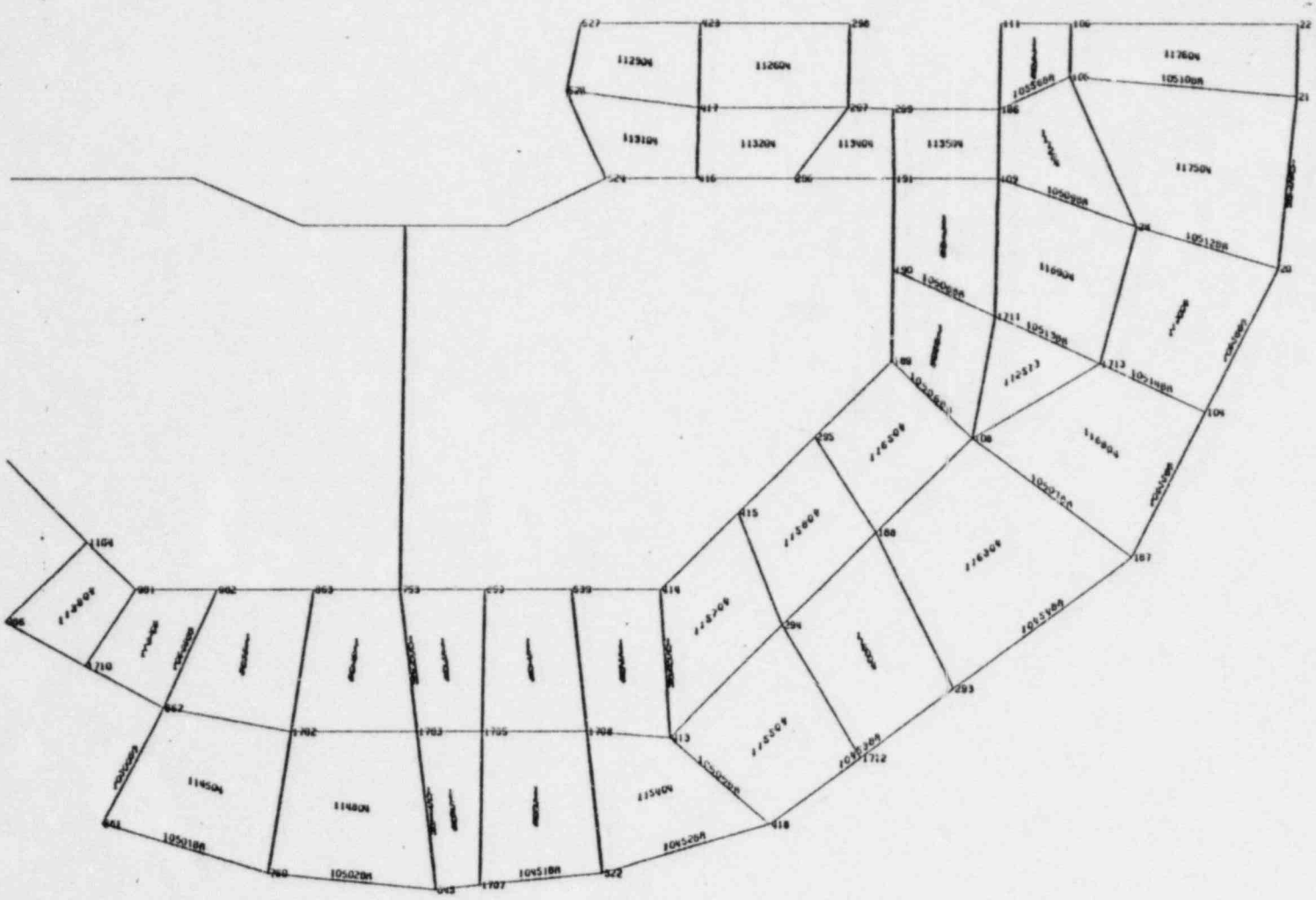

APPENDIX IV
FIG. 10

D.B. INTERNAL STRUCTURES
DIATIC ANALYSIS
UNDEFORMED SHAPE

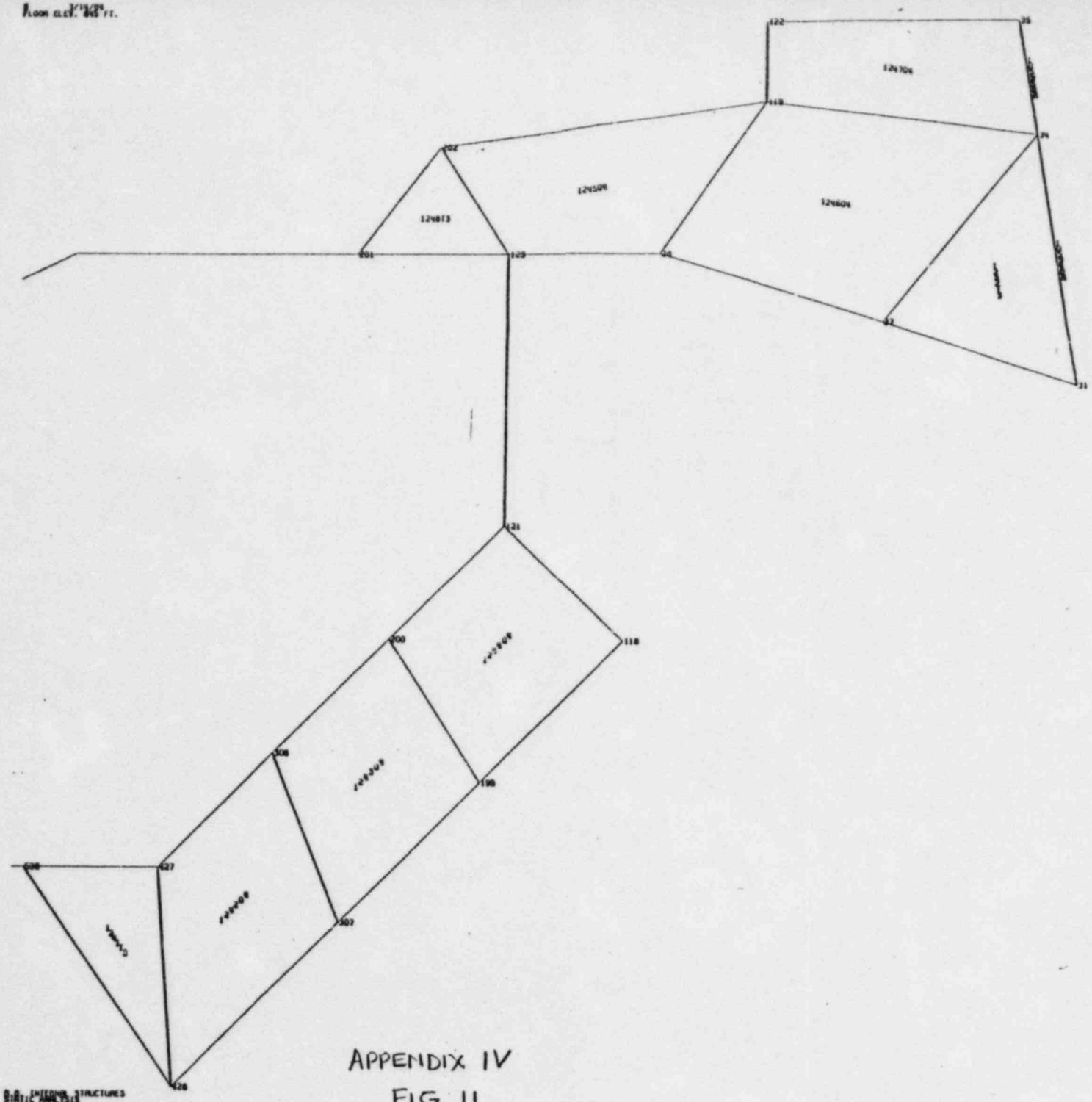

APPENDIX IV
FIG 11

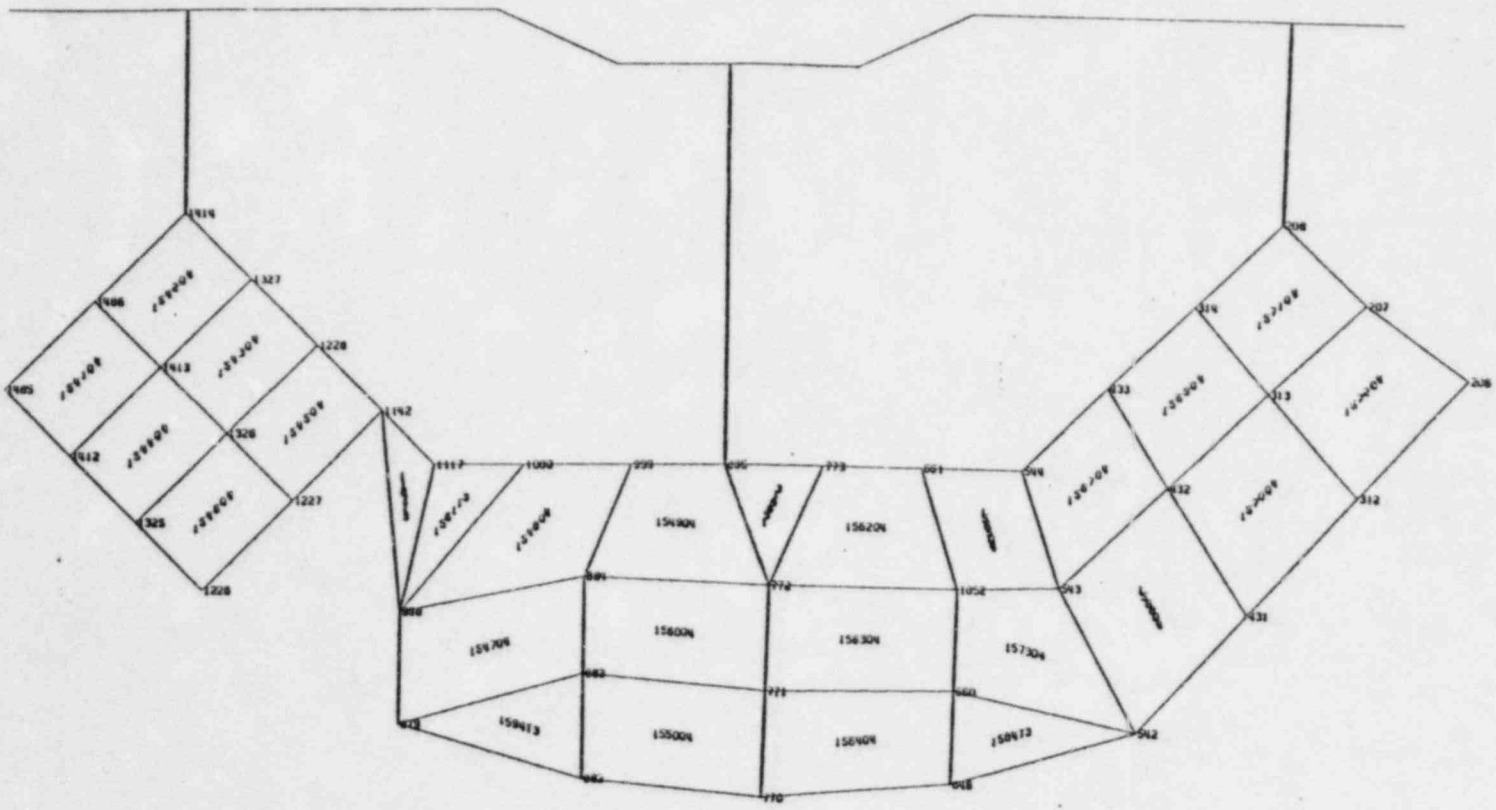

APPENDIX IV

FIG 12

GE INTERNAL STRUCTURES
STATIC ANALYSIS
UNDEFORMED SHAPE

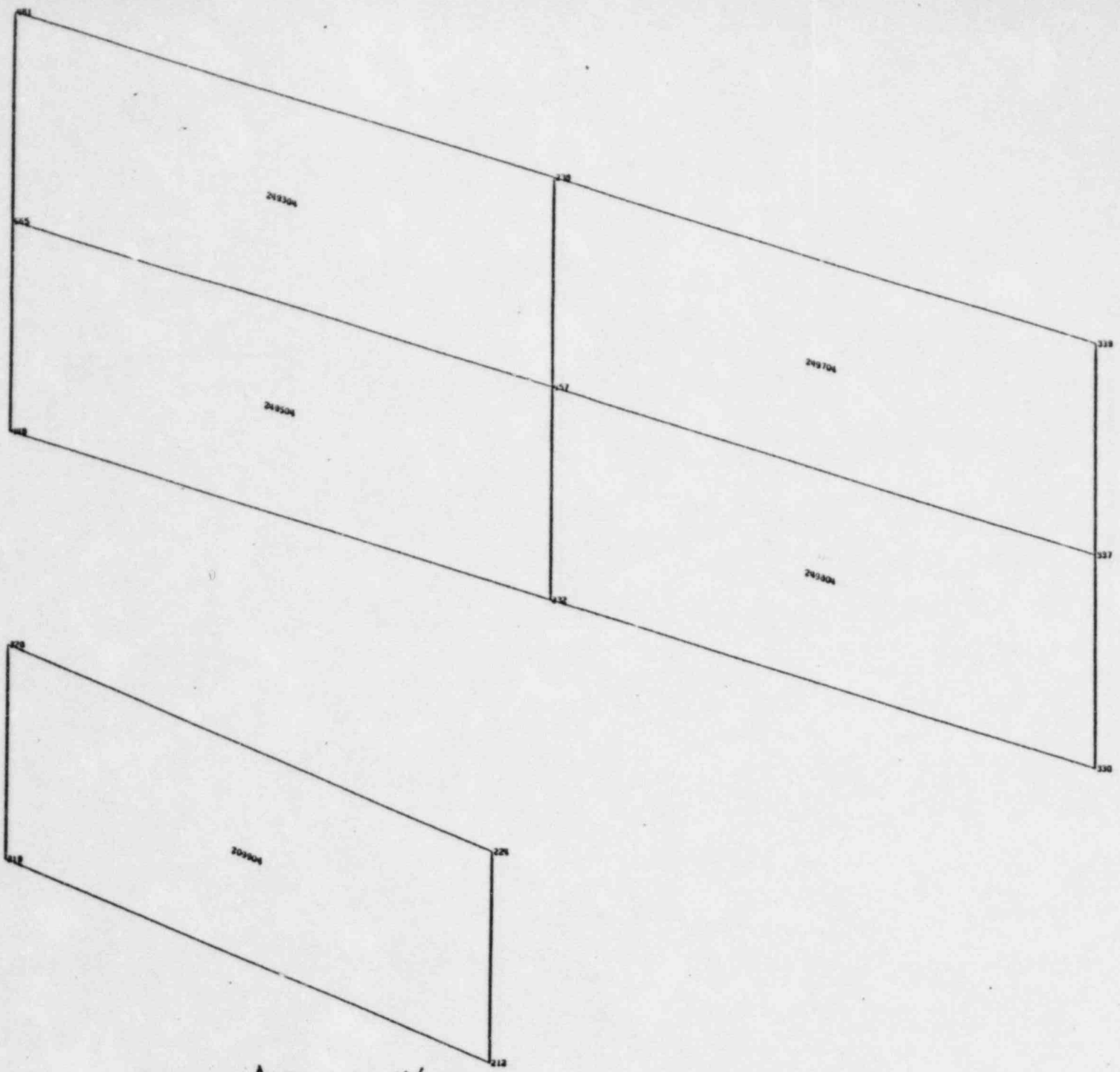

APPENDIX IV
FIG 13

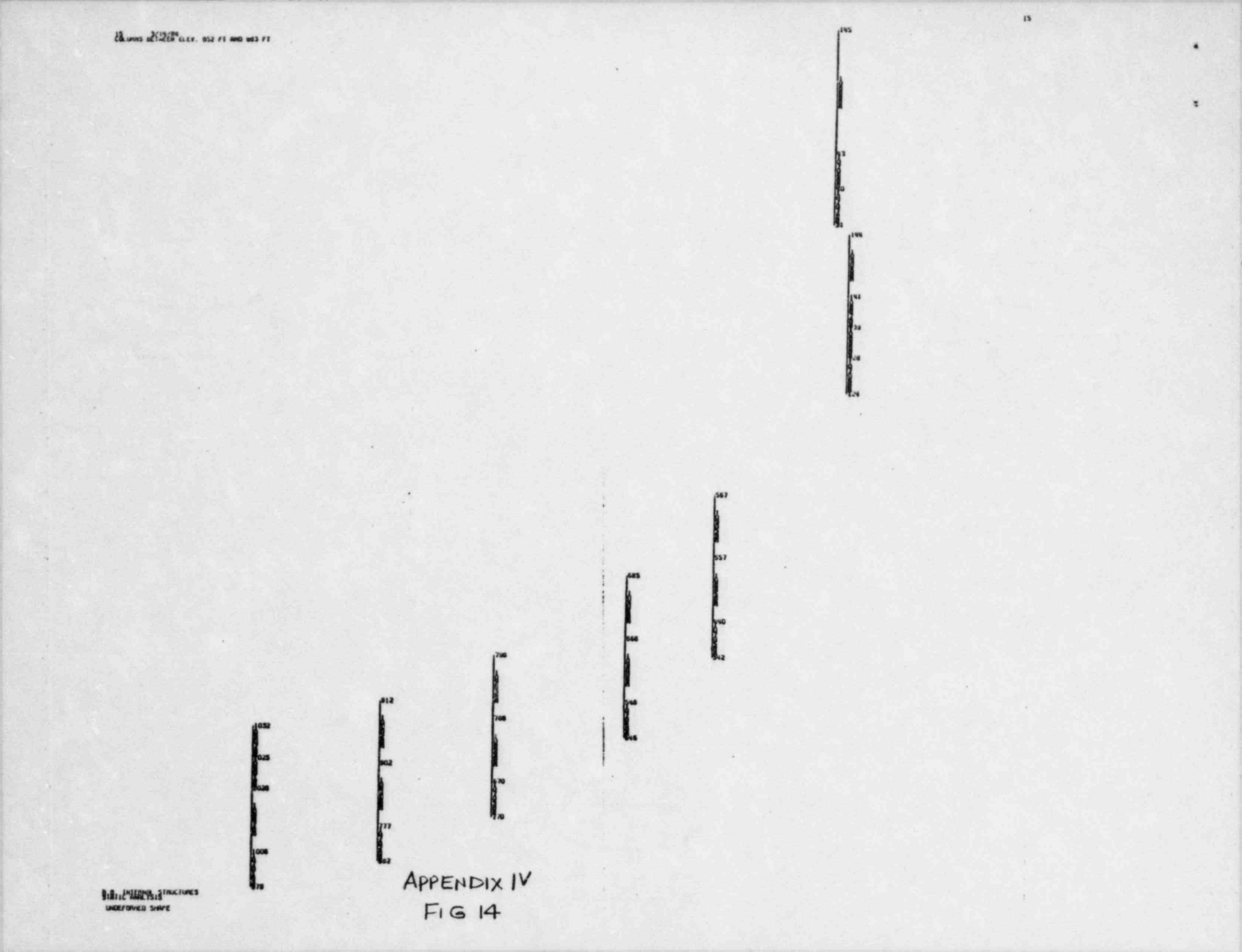

APPENDIX IV
FIG 14

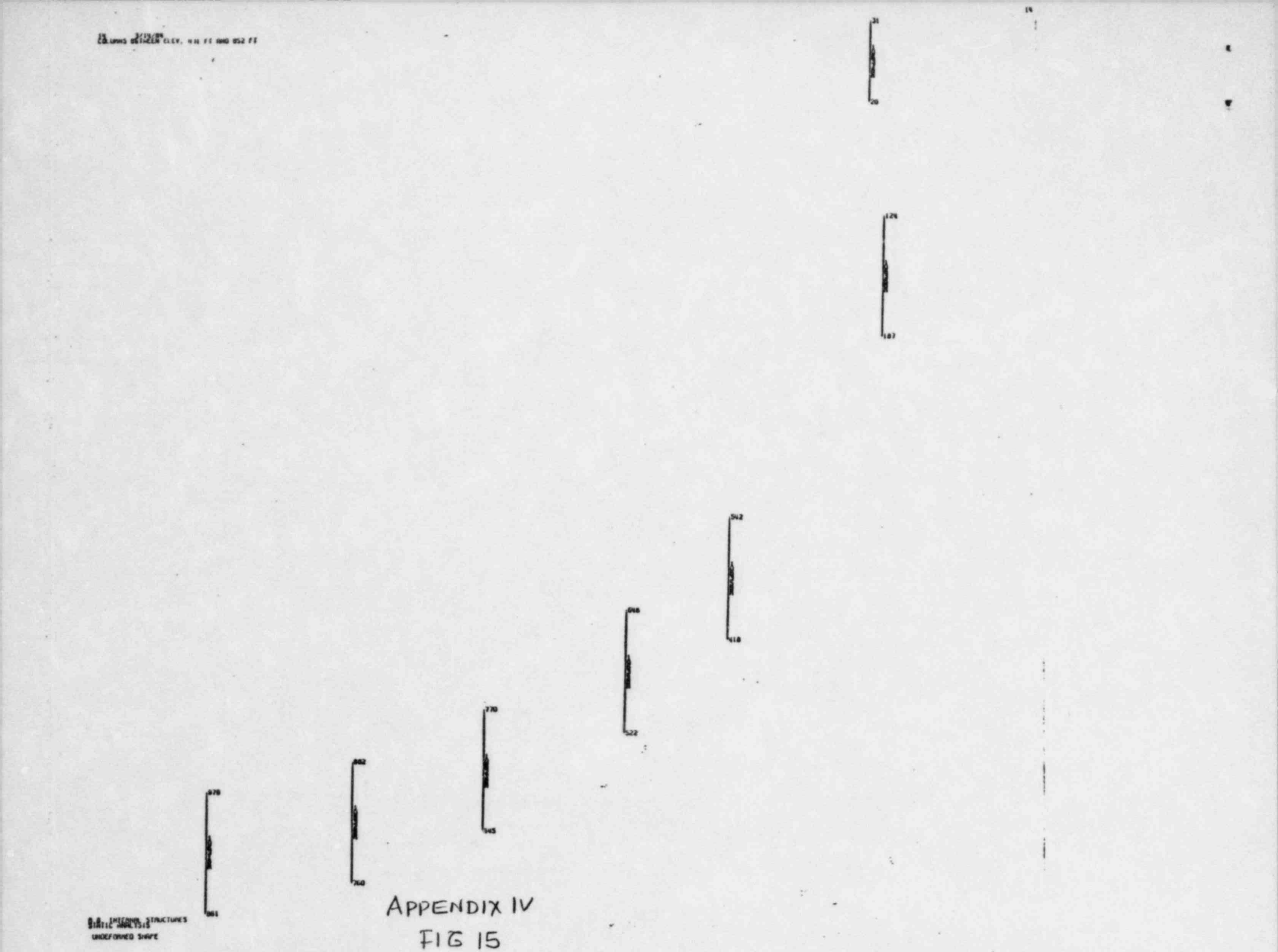

APPENDIX IV
FIG 15

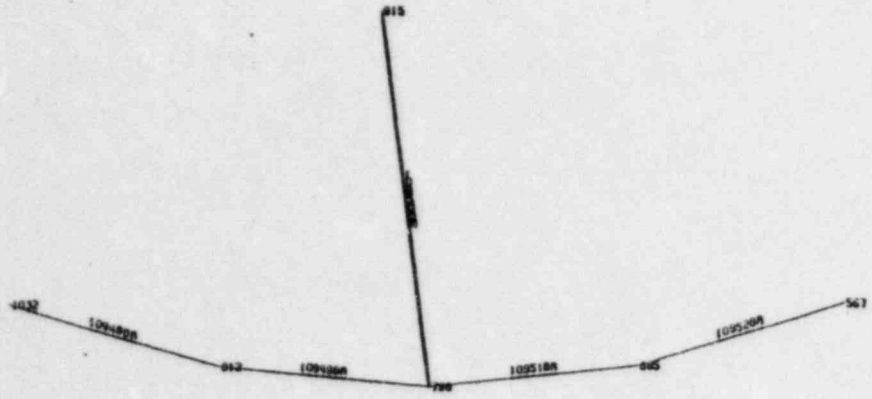

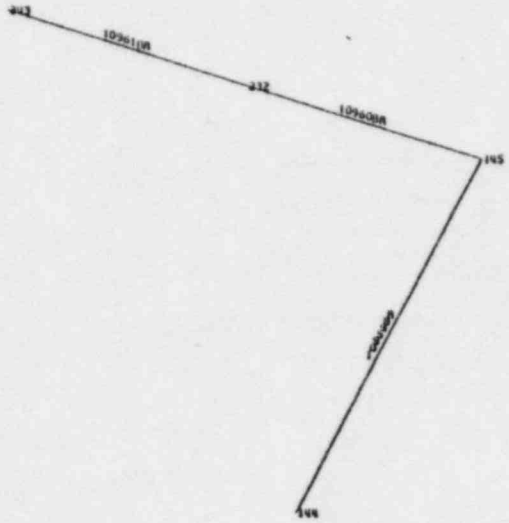

APPENDIX IV

FIG. 16

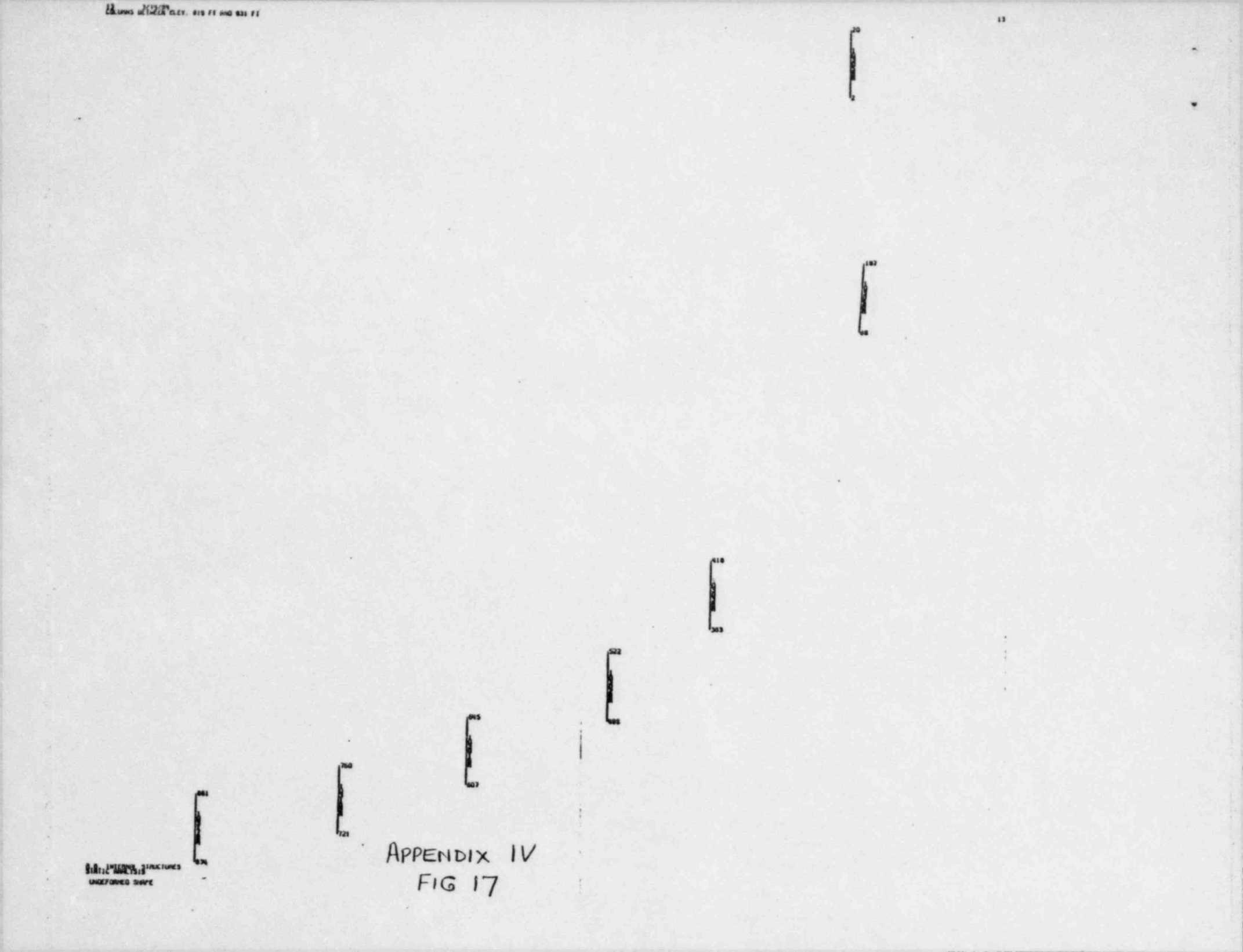

APPENDIX IV
FIG 17

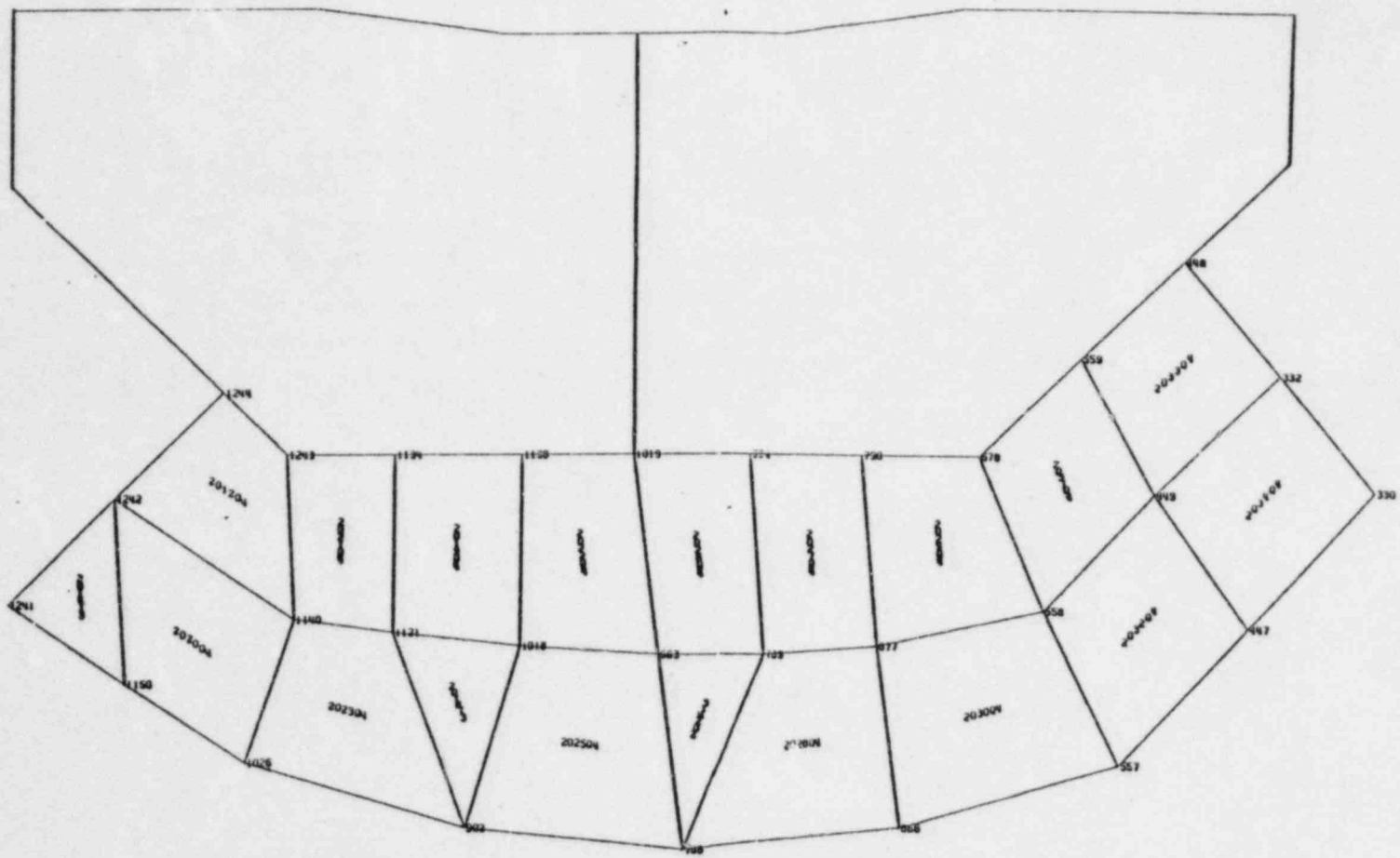

APPENDIX IV

FIG 18

S.A. ENTERPRISE STRUCTURES
STATIC ANALYSIS
UNDEFORMED SHAPE

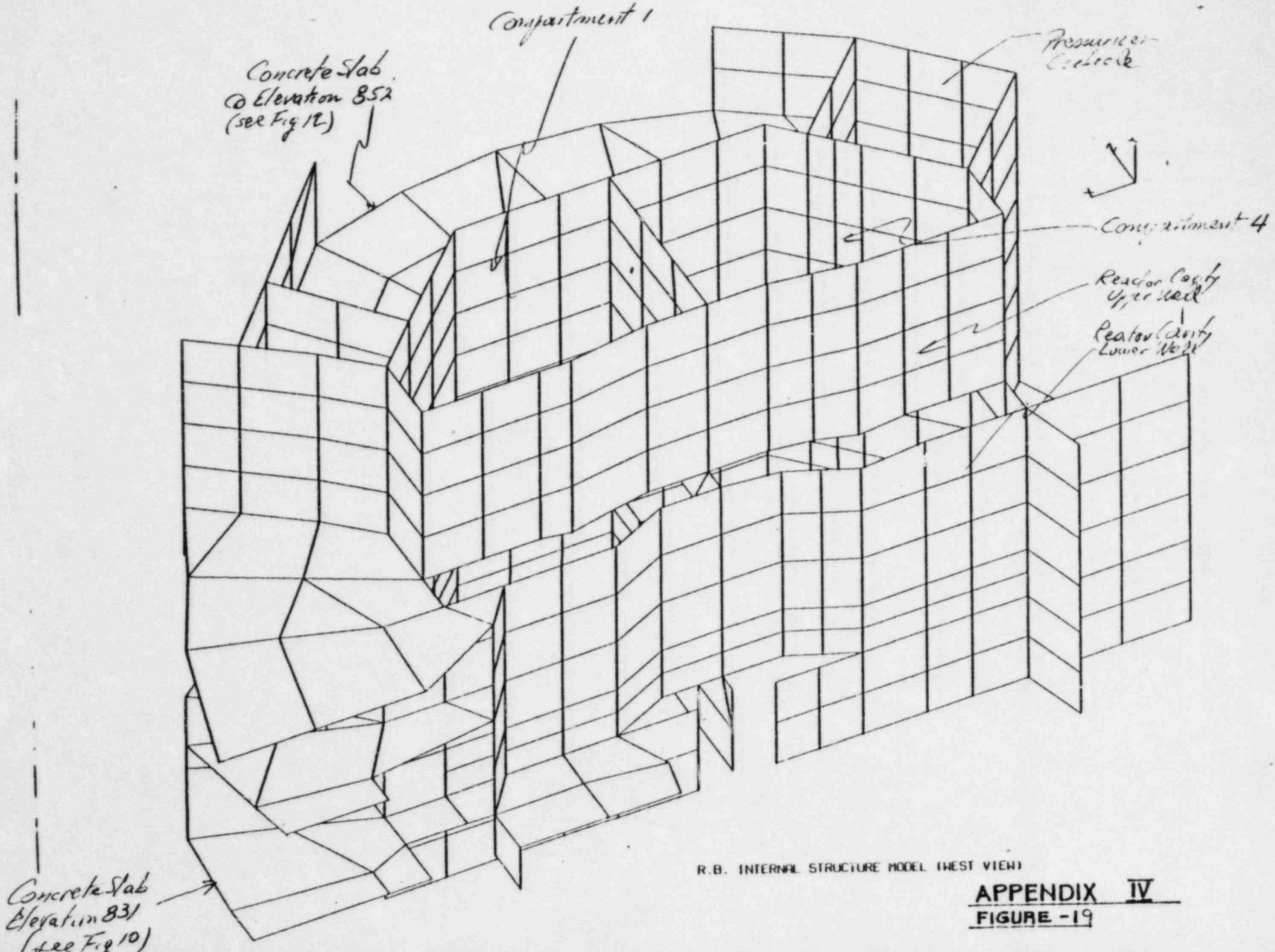

R.B. INTERNAL STRUCTURE MODEL (WEST VIEW)

APPENDIX IV
FIGURE -19

CONTAINMENT BUILDING
RELAP4 FLOW MODEL

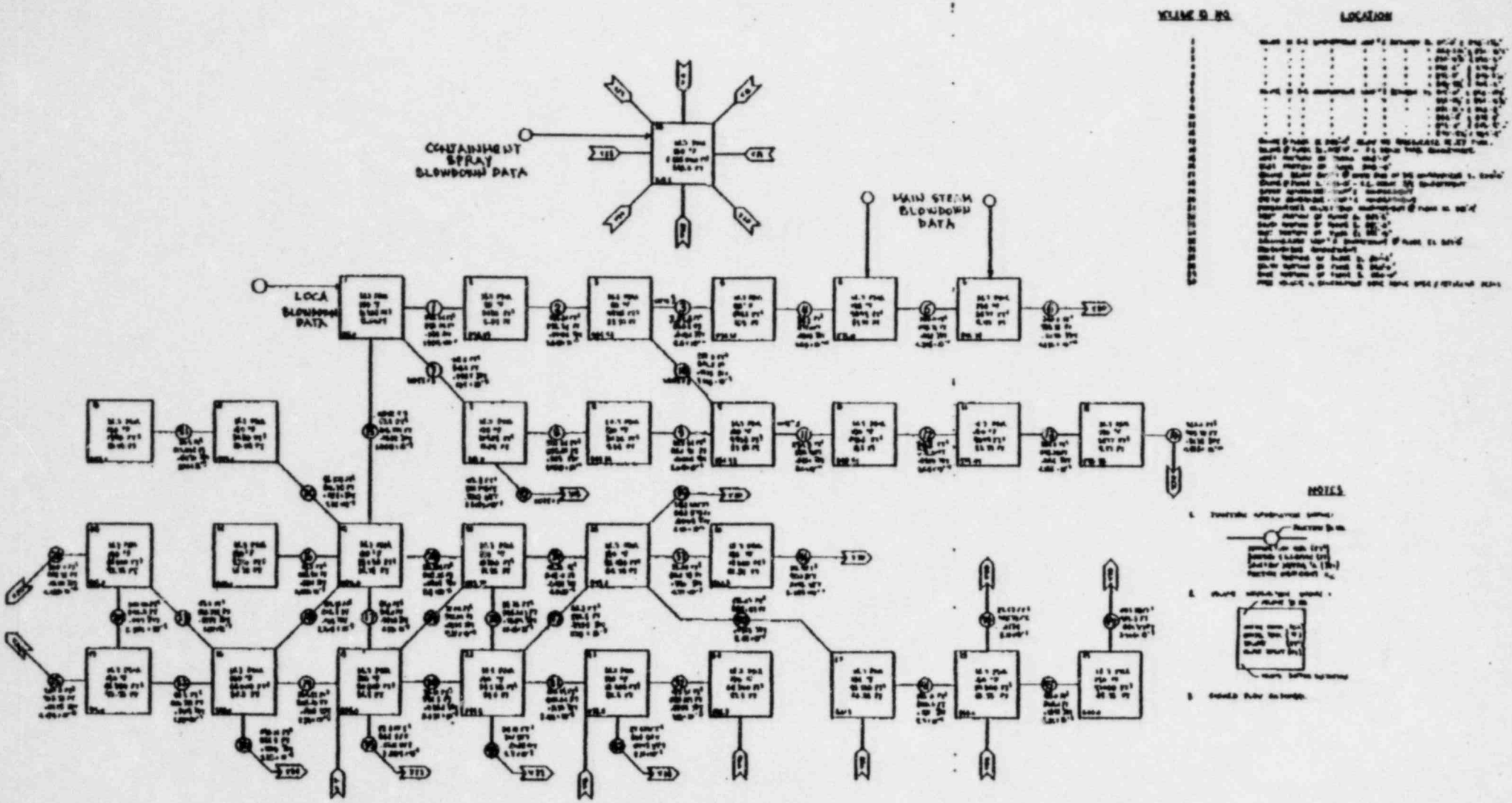

Appendix 5
Figure 1

Appendix 5
Figure 1

STEAM GENERATOR UPPER LATERAL SUPPORT BEAM HEATING5 MODEL

Appendix 5
Figure 2

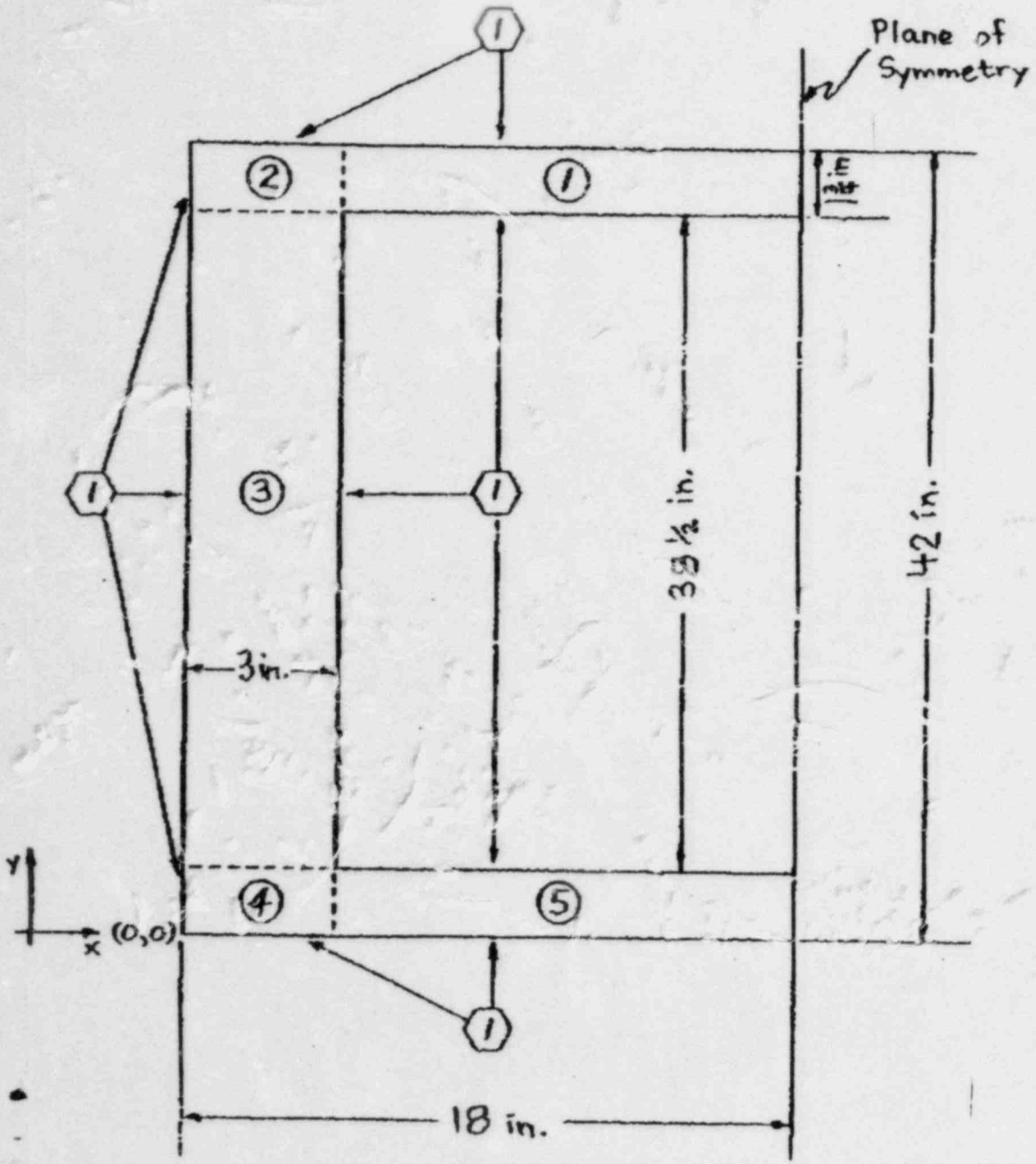

Since the beam is symmetric, only half of the beam cross-section was analyzed. The beam model consists of 5 regions.

Grid lines are placed at the following coordinates:

X: 0.0, 0.5, 1.0, 1.5, 2.0, 2.5, 3.0, 4.5, 6.0, 7.5, 9.0, 10.5, 12.0, 13.5, 15.0, 16.5, 18.0

Y: 0.0, 0.292, 0.583, 0.875, 1.167, 1.458, 1.75, 3.675, 5.6, 7.525, 9.45, 11.375, 13.3, 15.225, 17.15, 19.075, 21.0, 22.925, 24.85, 26.775, 28.7, 30.625, 32.55, 34.475, 36.4, 38.325, 40.25, 40.542, 40.833, 41.125, 41.417, 41.708, 42.0

LEGEND

○ Region Number
⬡ Boundary Number

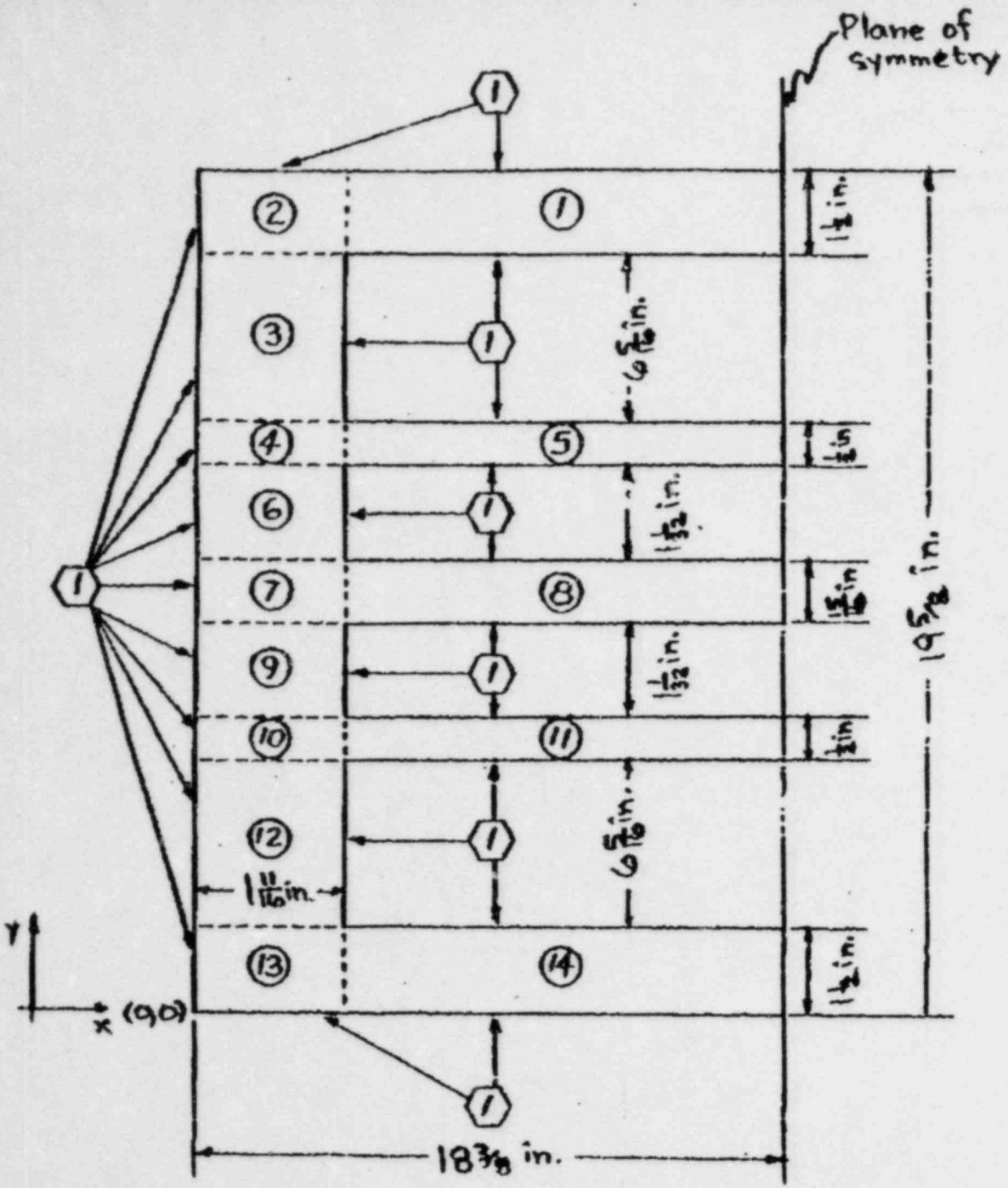

Appendix V Figure 3

Since the beam is symmetric, only half of the beam cross-section was analyzed. The beam model consists of 14 regions.

Grid lines are placed at the following coordinates:

X: 0.0, 0.25, 0.50, 0.75, 1.0, 1.25, 1.5, 1.6875, 2.53, 3.375, 4.875, 6.375, 7.875, 9.375, 10.875, 12.375, 13.875, 15.375, 16.875, 18.375

Y: 0.0, 0.25, 0.5, 0.75, 1.0, 1.25, 1.5, 2.25, 3.0, 4.5, 6.0, 6.906, 7.813, 7.938, 8.063, 8.188, 8.313, 8.828, 9.344, 9.578, 9.813, 10.047, 10.281, 10.797, 11.313, 11.438, 11.563, 11.689, 11.813, 12.719, 13.625, 15.125, 16.625, 17.375, 18.125, 18.375, 18.625, 18.875, 19.125, 19.375, 19.625

LEGEND

○ Region Number

⬡ Boundary Number